Photoproduction of φ and J/ψ meson off nucleon and nuclei

Sang-Ho Kim (金相鎬)

Soongsil University, Seoul, Republic of Korea
Origin of Matter and Evolution of Galaxies (OMEG) Institute

In collaboration with T.-S.H.Lee (ANL)

International Workshop on Quark Structure of Hadrons 2024
09 - 10 Aug, 2024, Riken, Japan

Contents

1. $\gamma\, p \to \varphi\, p$, $\gamma\, {}^4He \to \varphi\, {}^4He$
2. $\gamma\, p \to J/\psi\, p$, $\gamma\, A \to J/\psi\, A$ ($A = d, {}^4He, {}^{12}C, {}^{16}O, {}^{40}Ca$)

- ❑ Introduction
- ❑ Formalism
- ❑ Results
- ❑ Summary & Future work

Contents based on

a [S.H.Kim, T.-S.H.Lee, S.i.Nam, Y.Oh, PRC.104.045202 (2021)]

b [S.Sakinah, T.-S.H.Lee, H.M.Choi, PRC.109.065204 (2024)]

Contents

1. $\gamma\, p \rightarrow \varphi\, p$, $\gamma\, ^4\mathrm{He} \rightarrow \varphi\, ^4\mathrm{He}$

2. $\gamma\, p \rightarrow J/\psi\, p$, $\gamma\, A \rightarrow J/\psi\, A$ ($A = d$, ^{4}He, ^{12}C, ^{16}O, ^{40}Ca)

- ❑ Based on our dynamical reaction model (a), we will apply for the model (b) to make predictions for J/ψ photproduction for future experiments at EIC and JLab.
- ❑ We will improve the model (b) to relate the phenomenological c quark-nucleon potential to gluon GPD in nucleon, such that the gluon distributions in nuclei can be predicted for EIC experiments.

Contents based on

a [S.H.Kim, T.-S.H.Lee, S.i.Nam, Y.Oh, PRC.104.045202 (2021)]

b [S.Sakinah, T.-S.H.Lee, H.M.Choi, PRC.109.065204 (2024)]

□ Photoproduction of light vector mesons offers an ideal opportunity for studying gluonic interactions at high energies.
□ Pomeron exchange is responsible for describing slow rising total cross section.
□ The production mechanism at low energies should be investigated with the recent experimental data.

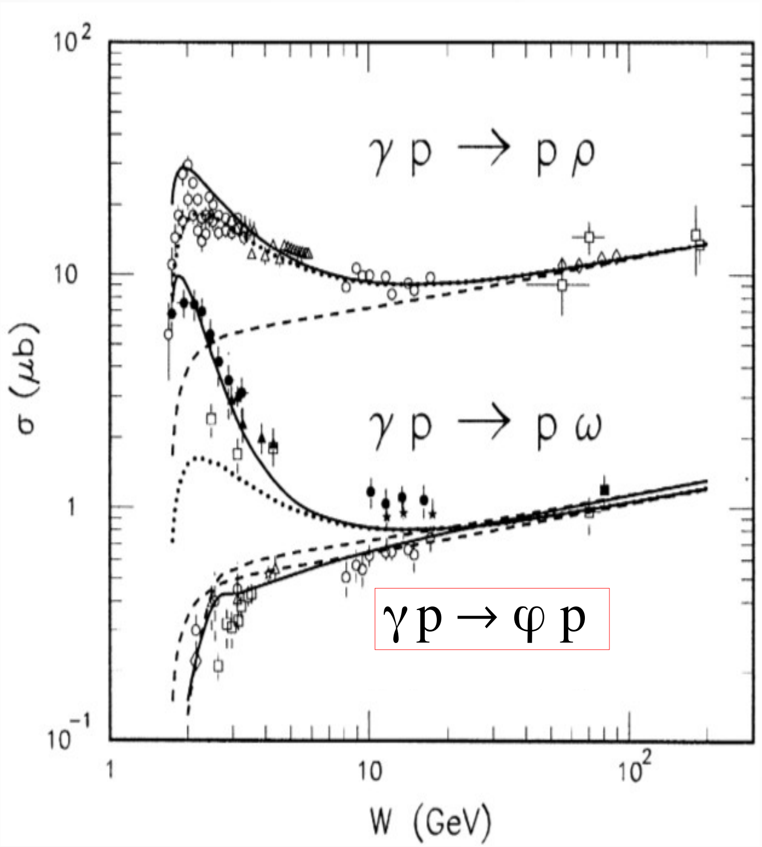

low energy : data [Dey, CLAS, PRC.89. 055208 (2014)
Seraydaryan, CLAS, PRC.89.055206 (2014)
Mizutani, LEPS, PRC.96.062201 (2017)]

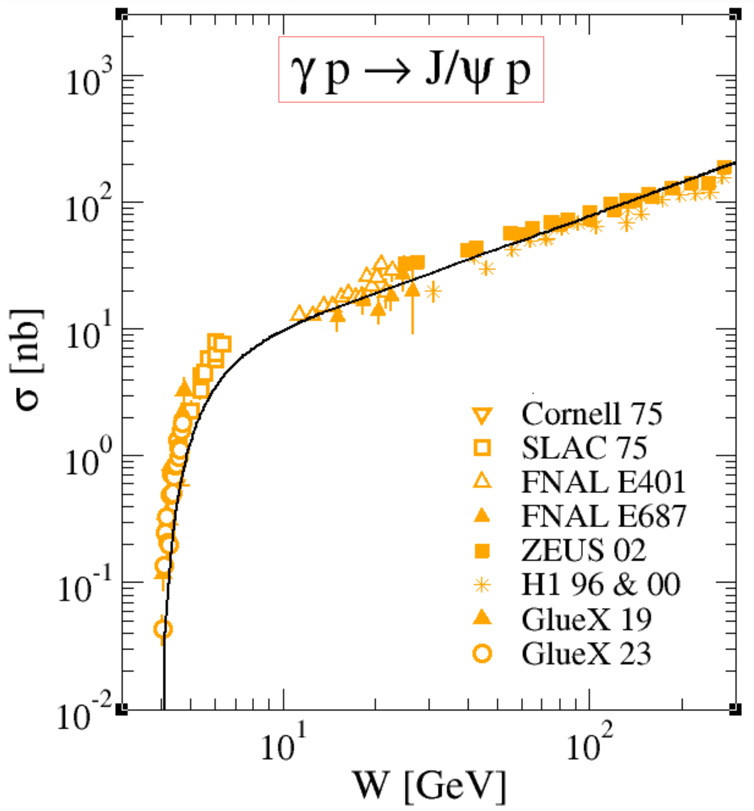

low energy : data [Pentchev, GlueX, PRL.123.072001 (2019)
Duran, JLab, Nature.615.813 (2023)
Pentchev, GlueX, PRC.108.025201 (2023)]

1. $\gamma\, p \rightarrow \varphi\, p, \quad \gamma\, {}^{4}He \rightarrow \varphi\, {}^{4}He$

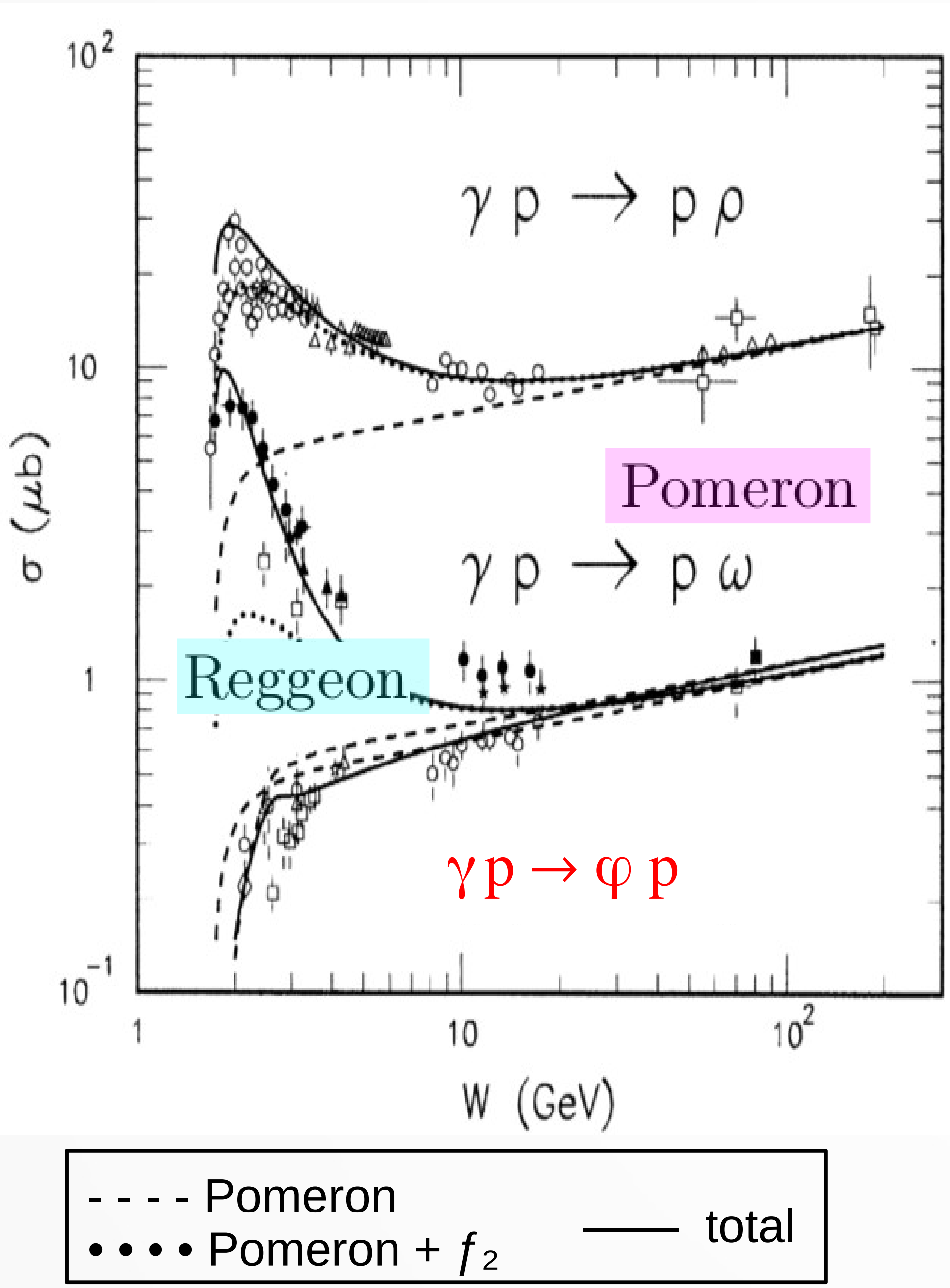

[Laget,PLB.489.313(2000)]

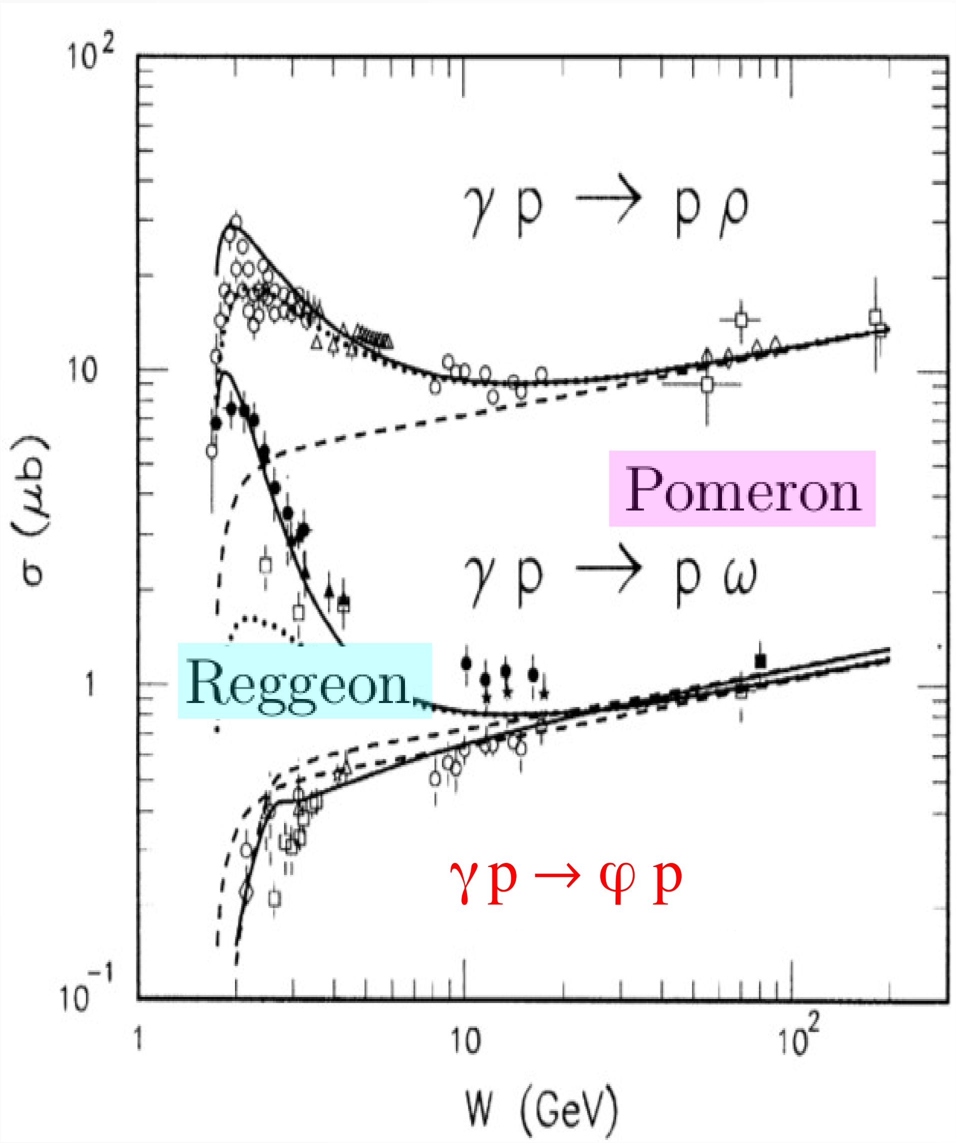

- - - - Pomeron
• • • • Pomeron + f_2
—— total

[Laget,PLB.489.313(2000)]

- We focus on γ p → φ p.
- high energy

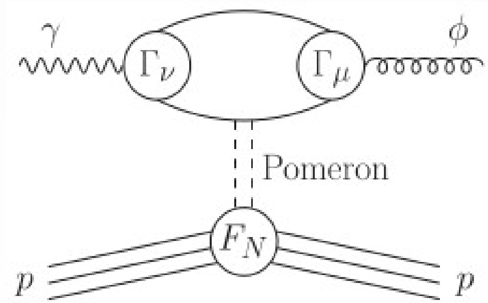

- σ [γp → φp] ≈ σ [γp → ωp]
- F_N: isoscalar EM form factor of the nucleon

$$F_N(t) = \frac{4M_N^2 - a_N^2 t}{(4M_N^2 - t)(1 - t/t_0)^2}$$

- $\alpha_P(t) = 1.08 + 0.25t$

- low energy

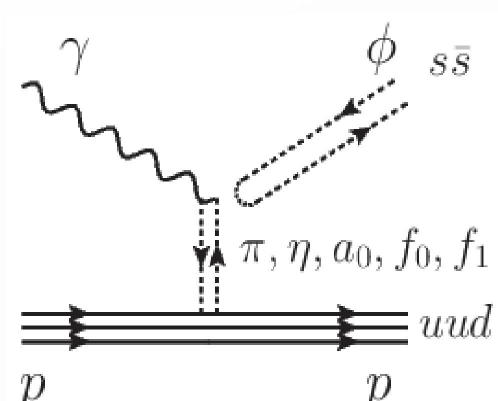

- σ[γp → φp] << σ[γp → (ρ,ω)p] due to the OZI rule

❑ high energy:

The two-gluon exchange is simplified by the Donnachie-Landshoff (DL) model which suggests that the Pomeron couples to the nucleon like a C = +1 isoscalar photon and its coupling is described in terms of $F_N(t)$.

[Pomeron Physics and QCD (Cambridge University, 2002)]

❑ low energy:

We need to clarify the reaction mechanism.

[Exp: Dey, CLAS, PRC.89. 055208 (2014)
Seraydaryan, CLAS, PRC.89.055206 (2014)
Mizutani, LEPS, PRC.96.062201 (2017)]

❑ We focus on γ p → φ p.

❑ high energy

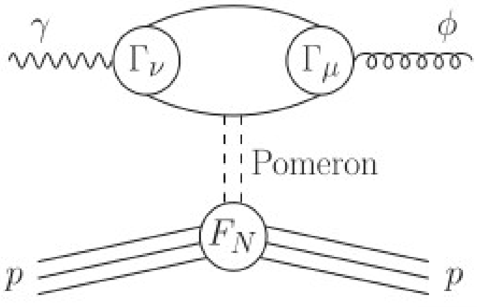

□ σ [γp → φp] ≈ σ [γp → ωp]

□ F_N: isoscalar EM form factor of the nucleon

$$F_N(t) = \frac{4M_N^2 - a_N^2 t}{(4M_N^2 - t)(1 - t/t_0)^2}$$

□ $\alpha_P(t) = 1.08 + 0.25t$

❑ low energy

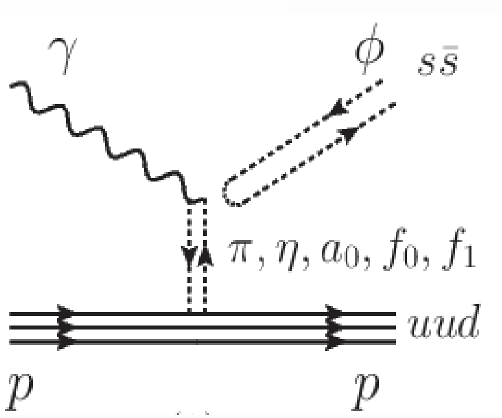

□ σ[γp → φp] << σ[γp → (ρ,ω)p] due to the OZI rule

Born term

❑ Scattering amplitude: $T_{\phi N,\gamma N}(E) = [B_{\phi N,\gamma N} \quad]$

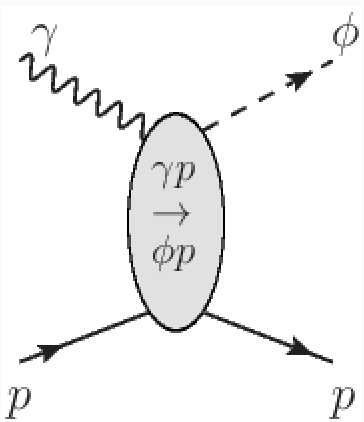

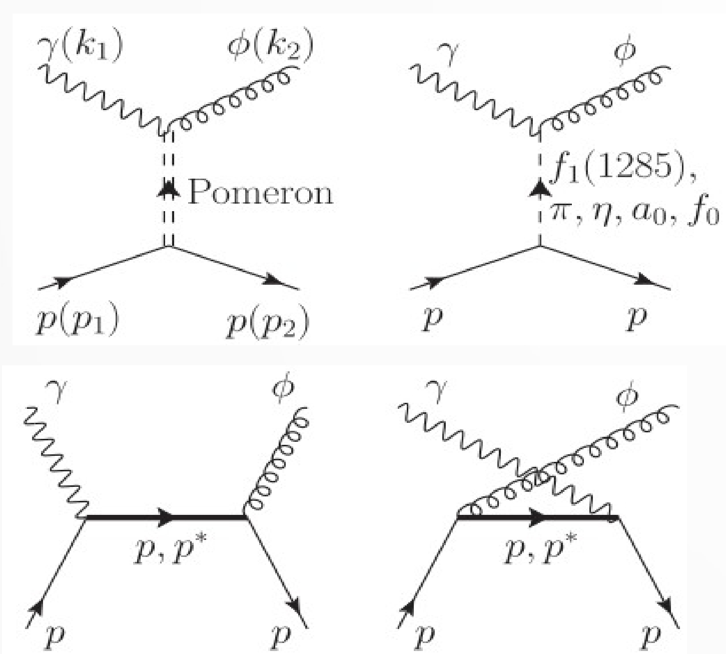

□ Ward-Takahashi identity

$$\mathcal{M}(k) = \epsilon_\mu(k)\mathcal{M}^\mu(k)$$

if we replace ϵ_μ with k_μ:

$$k_\mu \mathcal{M}^\mu(k) = 0$$

Born term

❑ Scattering amplitude: $T_{\phi N,\gamma N}(E) = [B_{\phi N,\gamma N} \qquad]$

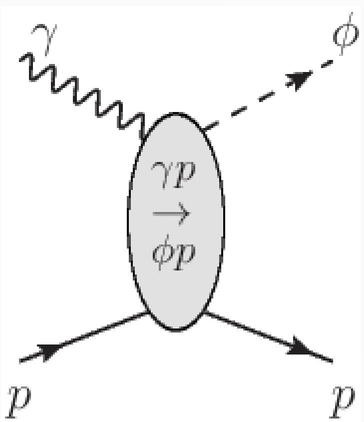

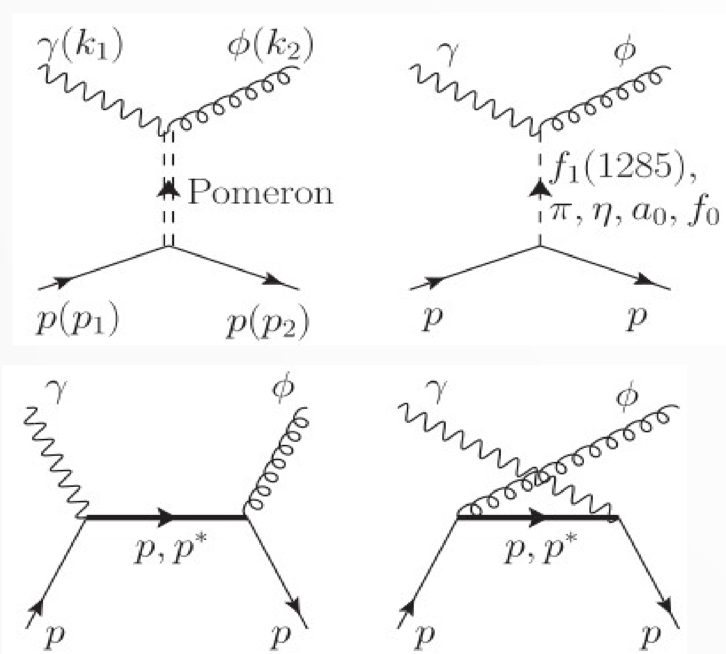

❑ Effective Lagrangians

□ EM vertex

$$\mathcal{L}_{\gamma\phi f_1} = g_{\gamma\phi f_1}\epsilon^{\mu\nu\alpha\beta}\partial_\mu A_\nu \partial^\lambda\partial_\lambda \phi_\alpha f_{1\beta}$$

$$\mathcal{L}_{\gamma\Phi\phi} = \frac{e g_{\gamma\Phi\phi}}{M_\phi}\epsilon^{\mu\nu\alpha\beta}\partial_\mu A_\nu \partial_\alpha \phi_\beta \Phi$$

$$\mathcal{L}_{\gamma S\phi} = \frac{e g_{\gamma S\phi}}{M_\phi} F^{\mu\nu}\phi_{\mu\nu} S$$

□ strong vertex

$$\mathcal{L}_{f_1 NN} = -g_{f_1 NN}\bar{N}\left[\gamma_\mu - i\frac{\kappa_{f_1 NN}}{2M_N}\gamma_\nu\gamma_\mu\partial^\nu\right] f_1^\mu \gamma_5 N$$

$$\mathcal{L}_{\Phi NN} = -i g_{\Phi NN}\bar{N}\Phi\gamma_5 N$$

$$\mathcal{L}_{SNN} = -g_{SNN}\bar{N} S N$$

$$\mathcal{L}_{\gamma NN} = -e\bar{N}\left[\gamma_\mu - \frac{\kappa_N}{2M_N}\sigma_{\mu\nu}\partial^\nu\right] N A^\mu$$

$$\mathcal{L}_{\phi NN} = -g_{\phi NN}\bar{N}\left[\gamma_\mu - \frac{\kappa_{\phi NN}}{2M_N}\sigma_{\mu\nu}\partial^\nu\right] N \phi^\mu$$

Born term

❑ Scattering amplitude: $T_{\phi N,\gamma N}(E) = [B_{\phi N,\gamma N} \quad]$

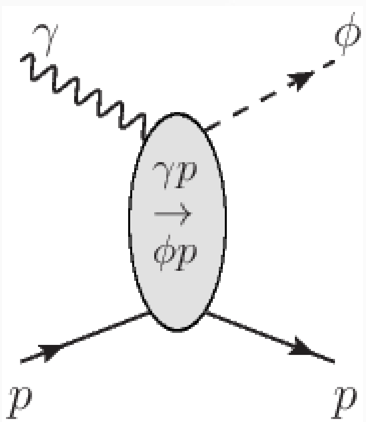

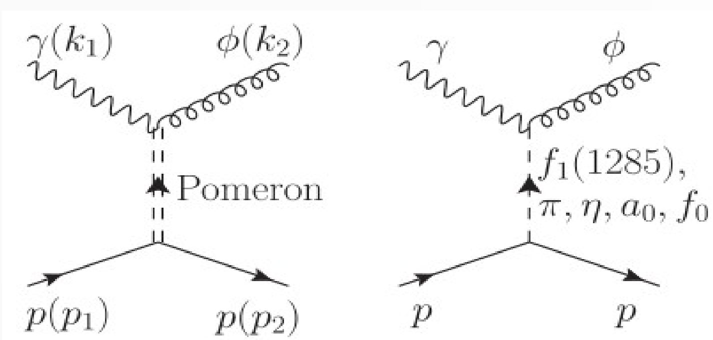

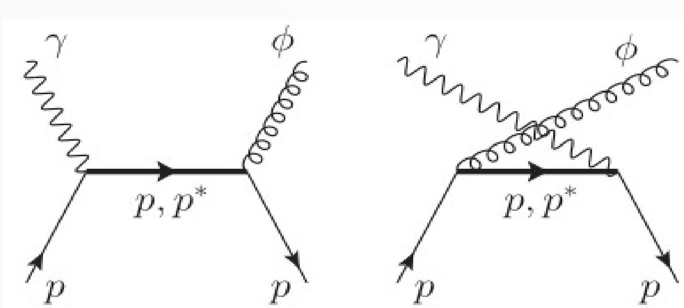

$$\mathcal{M} = \varepsilon^*_\nu \bar{u}_{N'} \mathcal{M}^{\mu\nu} u_N \epsilon_\mu$$

$$\mathcal{M}^{\mu\nu}_{f_1} = i\frac{M^2_\phi g_{\gamma f_1 \phi} g_{f_1 NN}}{t - M^2_{f_1}} \epsilon^{\mu\nu\alpha\beta}\left[-g_{\alpha\lambda} + \frac{q_{t\alpha} q_{t\lambda}}{M^2_{f_1}}\right] \times \left[\gamma^\lambda + \frac{\kappa_{f_1 NN}}{2M_N}\gamma^\sigma\gamma^\lambda q_{t\sigma}\right]\gamma_5 k_{1\beta},$$

$$\mathcal{M}^{\mu\nu}_{\Phi} = i\frac{e}{M_\phi}\frac{g_{\gamma\Phi\phi} g_{\Phi NN}}{t - M^2_\Phi}\epsilon^{\mu\nu\alpha\beta} k_{1\alpha} k_{2\beta}\gamma_5,$$

$$\mathcal{M}^{\mu\nu}_{S} = \frac{e}{M_\phi}\frac{2 g_{\gamma S\phi} g_{SNN}}{t - M^2_S + i\Gamma_S M_S}(k_1 k_2 g^{\mu\nu} - k^\mu_1 k^\nu_2),$$

$$\mathcal{M}^{\mu\nu}_{\phi\,\mathrm{rad},s} = \frac{e g_{\phi NN}}{s - M^2_N}\left(\gamma^\nu - i\frac{\kappa_{\phi NN}}{2M_N}\sigma^{\nu\alpha} k_{2\alpha}\right)(\not{q}_s + M_N) \times \left(\gamma^\mu + i\frac{\kappa_N}{2M_N}\sigma^{\mu\beta} k_{1\beta}\right),$$

$$\mathcal{M}^{\mu\nu}_{\phi\,\mathrm{rad},u} = \frac{e g_{\phi NN}}{u - M^2_N}\left(\gamma^\mu + i\frac{\kappa_N}{2M_N}\sigma^{\mu\alpha} k_{1\alpha}\right)(\not{q}_u + M_N) \times \left(\gamma^\nu - i\frac{\kappa_{\phi NN}}{2M_N}\sigma^{\nu\beta} k_{2\beta}\right),$$

❑ Effective Lagrangians

□ EM vertex

$$\mathcal{L}_{\gamma\phi f_1} = g_{\gamma\phi f_1}\epsilon^{\mu\nu\alpha\beta}\partial_\mu A_\nu \partial^\lambda \partial_\lambda \phi_\alpha f_{1\beta}$$

$$\mathcal{L}_{\gamma\Phi\phi} = \frac{e g_{\gamma\Phi\phi}}{M_\phi}\epsilon^{\mu\nu\alpha\beta}\partial_\mu A_\nu \partial_\alpha \phi_\beta \Phi$$

$$\mathcal{L}_{\gamma S\phi} = \frac{e g_{\gamma S\phi}}{M_\phi} F^{\mu\nu}\phi_{\mu\nu} S$$

□ strong vertex

$$\mathcal{L}_{f_1 NN} = -g_{f_1 NN}\bar{N}\left[\gamma_\mu - i\frac{\kappa_{f_1 NN}}{2M_N}\gamma_\nu\gamma_\mu\partial^\nu\right] f^\mu_1 \gamma_5 N$$

$$\mathcal{L}_{\Phi NN} = -i g_{\Phi NN}\bar{N}\Phi\gamma_5 N$$

$$\mathcal{L}_{SNN} = -g_{SNN}\bar{N} S N$$

$$\mathcal{L}_{\gamma NN} = -e\bar{N}\left[\gamma_\mu - \frac{\kappa_N}{2M_N}\sigma_{\mu\nu}\partial^\nu\right] N A^\mu$$

$$\mathcal{L}_{\phi NN} = -g_{\phi NN}\bar{N}\left[\gamma_\mu - \frac{\kappa_{\phi NN}}{2M_N}\sigma_{\mu\nu}\partial^\nu\right] N \phi^\mu$$

final state interaction (FSI)

❑ Scattering amplitude: $T_{\phi N,\gamma N}(E) = [B_{\phi N,\gamma N} + T^{FSI}_{\phi N,\gamma N}(E)]$

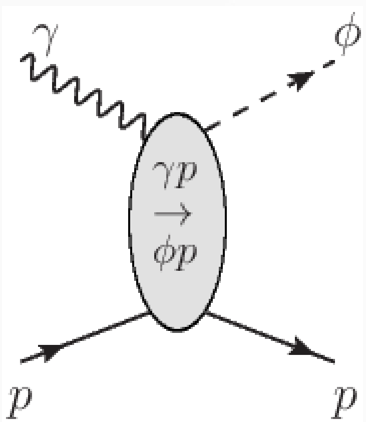

+

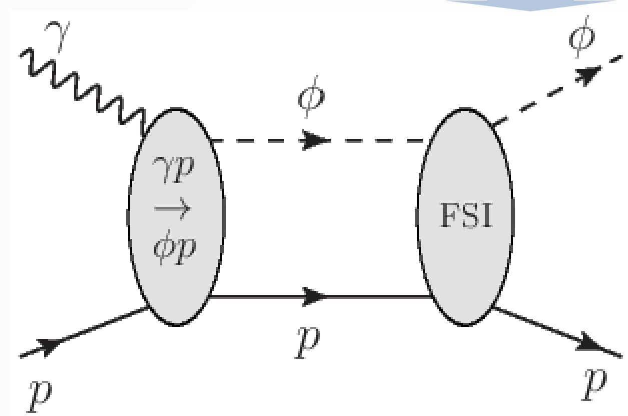

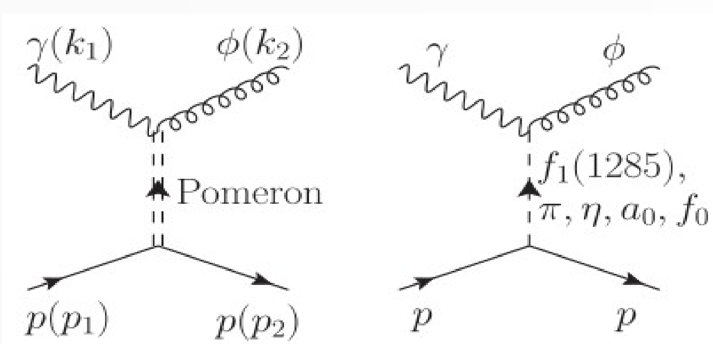

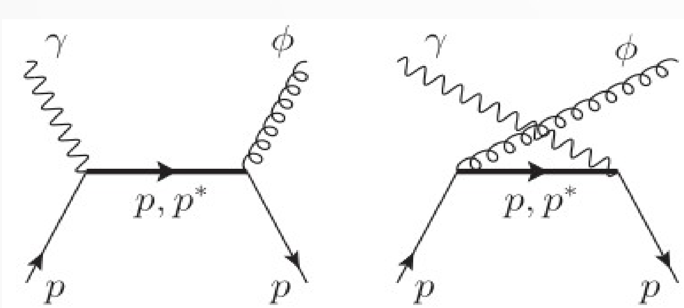

FSI=

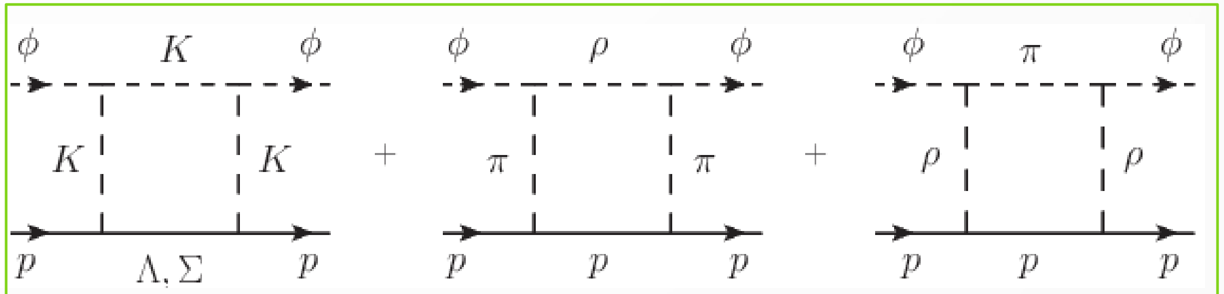

□ decay mode of φ-meson

Γ_1	K^+K^-	$(49.2 \pm 0.5)\%$
Γ_2	$K^0_L K^0_S$	$(34.0 \pm 0.4)\%$
Γ_3	$\rho\pi + \pi^+\pi^-\pi^0$	$(15.24 \pm 0.33)\%$
Γ_4	$\rho\pi$	
Γ_5	$\pi^+\pi^-\pi^0$	
Γ_6	$\eta\gamma$	$(1.303 \pm 0.025)\%$
Γ_7	$\pi^0\gamma$	$(1.32 \pm 0.06) \times 10^{-3}$
Γ_8	$\ell^+\ell^-$	
Γ_9	e^+e^-	$(2.974 \pm 0.034) \times 10^{-4}$
Γ_{10}	$\mu^+\mu^-$	$(2.86 \pm 0.19) \times 10^{-4}$
Γ_{11}	ηe^+e^-	$(1.08 \pm 0.04) \times 10^{-4}$
Γ_{12}	$\pi^+\pi^-$	$(7.3 \pm 1.3) \times 10^{-5}$
Γ_{13}	$\omega\pi^0$	$(4.7 \pm 0.5) \times 10^{-5}$
Γ_{14}	$\omega\gamma$	$< 5\%$
Γ_{15}	$\rho\gamma$	$< 1.2 \times 10^{-5}$

final state interaction (FSI)

❑ Scattering amplitude: $T_{\phi N,\gamma N}(E) = [B_{\phi N,\gamma N} + T^{FSI}_{\phi N,\gamma N}(E)]$

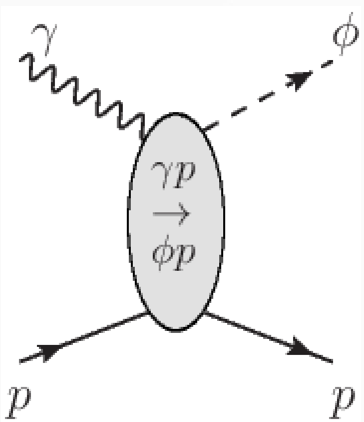

+

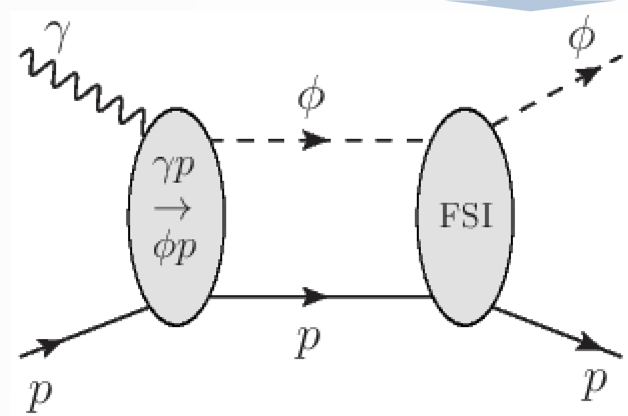

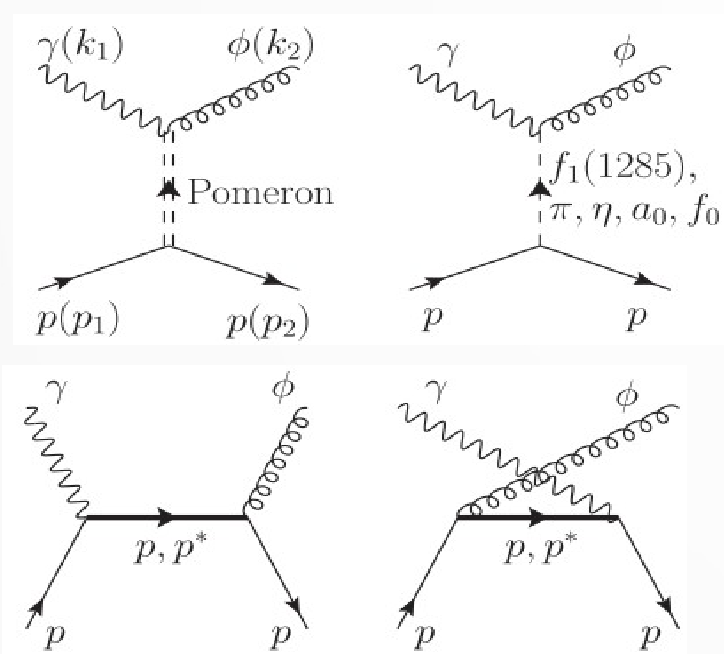

FSI=

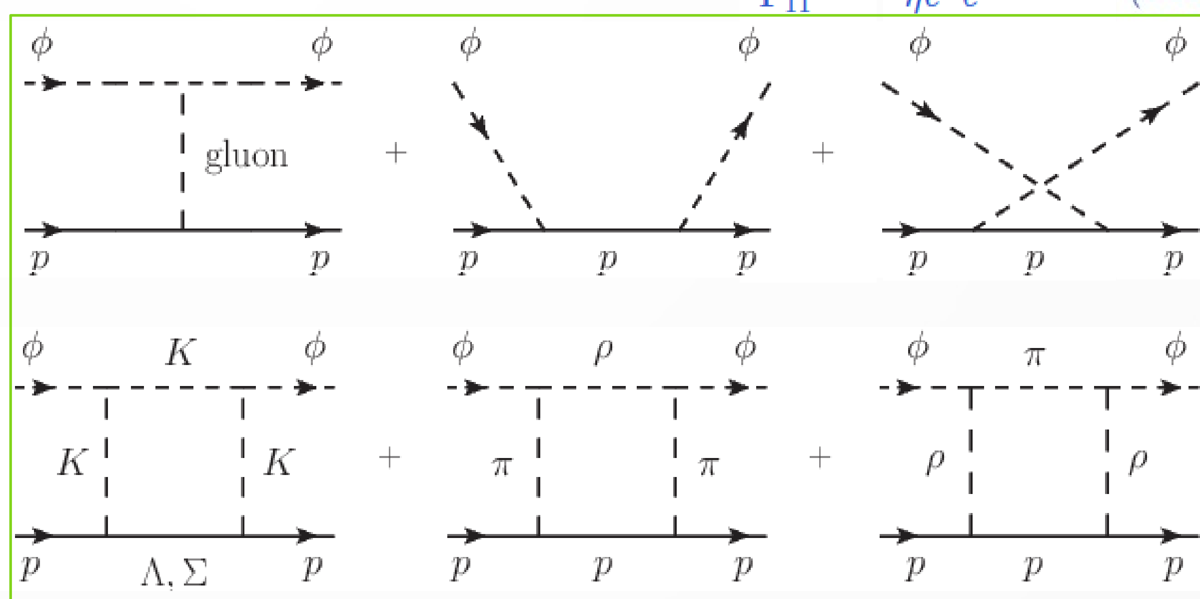

□ decay mode of φ-meson

Γ_1	$K^+ K^-$	$(49.2 \pm 0.5)\%$
Γ_2	$K^0_L\ K^0_S$	$(34.0 \pm 0.4)\%$
Γ_3	$\rho\pi + \pi^+\pi^-\pi^0$	$(15.24 \pm 0.33)\%$
Γ_4	$\rho\pi$	
Γ_5	$\pi^+\pi^-\pi^0$	
Γ_6	$\eta\gamma$	$(1.303 \pm 0.025)\%$
Γ_7	$\pi^0\gamma$	$(1.32 \pm 0.06) \times 10^{-3}$
Γ_8	$\ell^+\ell^-$	
Γ_9	e^+e^-	$(2.974 \pm 0.034) \times 10^{-4}$
Γ_{10}	$\mu^+\mu^-$	$(2.86 \pm 0.19) \times 10^{-4}$
Γ_{11}	$\eta e^+ e^-$	$(1.08 \pm 0.04) \times 10^{-4}$
		$1.3) \times 10^{-5}$
		$0.5) \times 10^{-5}$
		$\times 10^{-5}$

final state interaction (FSI)

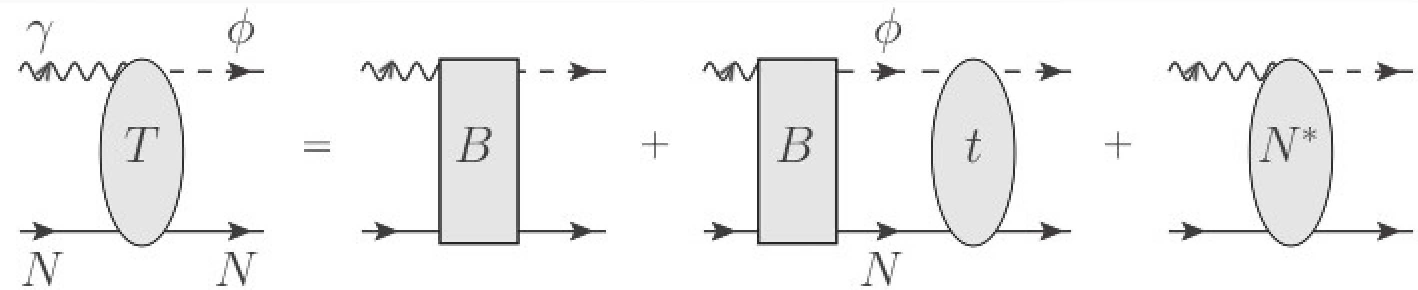

$$T_{\phi N,\gamma N}(E) = B_{\phi N,\gamma N} + T^{\rm FSI}_{\phi N,\gamma N}(E) + T^{N^*}_{\phi N,\gamma N}(E)$$

$t_{\phi N,\phi N}(E)$

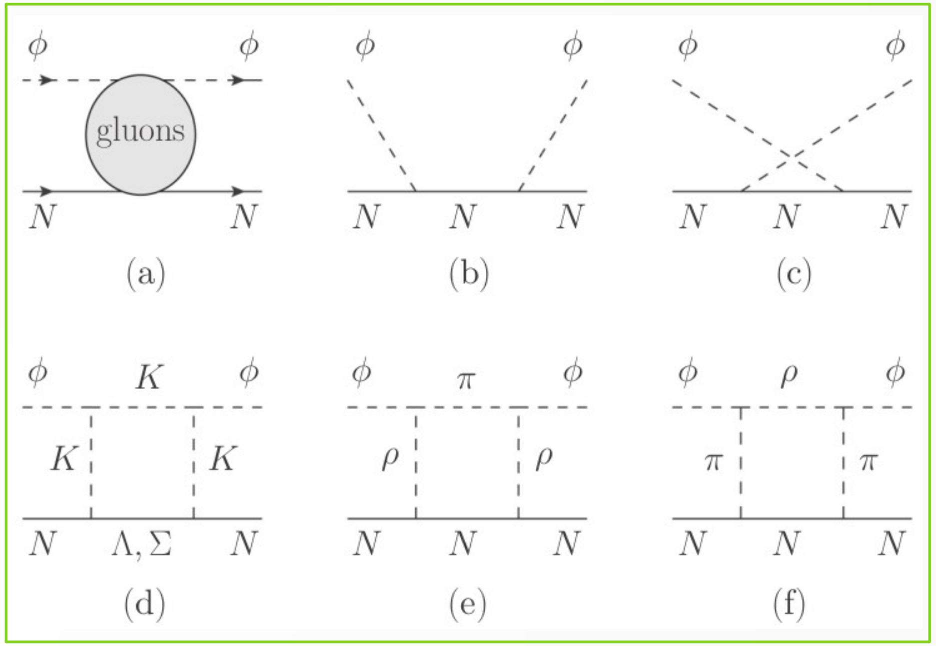

final state interaction (FSI)

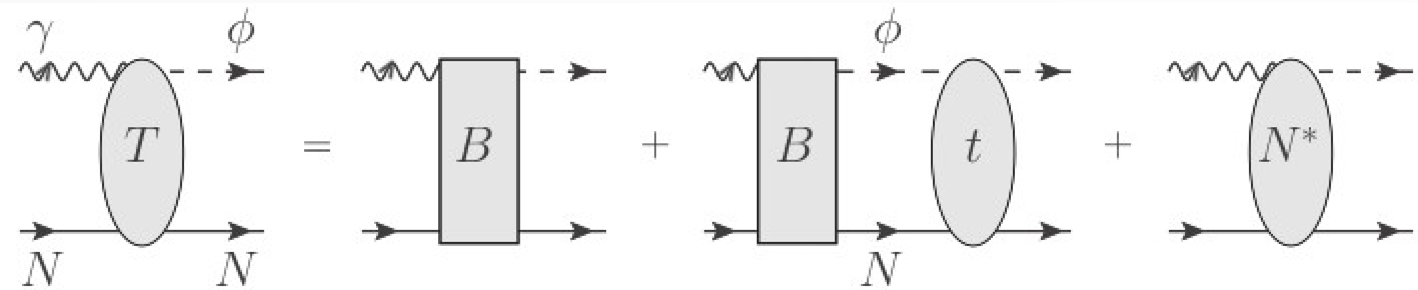

$$T_{\phi N,\gamma N}(E) = B_{\phi N,\gamma N} + T^{\mathrm{FSI}}_{\phi N,\gamma N}(E) + T^{N^*}_{\phi N,\gamma N}(E)$$

$$t_{\phi N,\phi N}(E) G_{\phi N}(E) B_{\phi N,\gamma N}$$

$$G_{MB}(E) = \frac{|MB\rangle\langle MB|}{E - H_0 + i\epsilon}$$: meson-baryon propagator

$$t_{\phi N,\phi N}(E) = V_{\phi N,\phi N}(E) + V_{\phi N,\phi N} G_{\phi N}(E) t_{\phi N,\phi N}(E)$$

$t_{\phi N,\phi N}(E)$

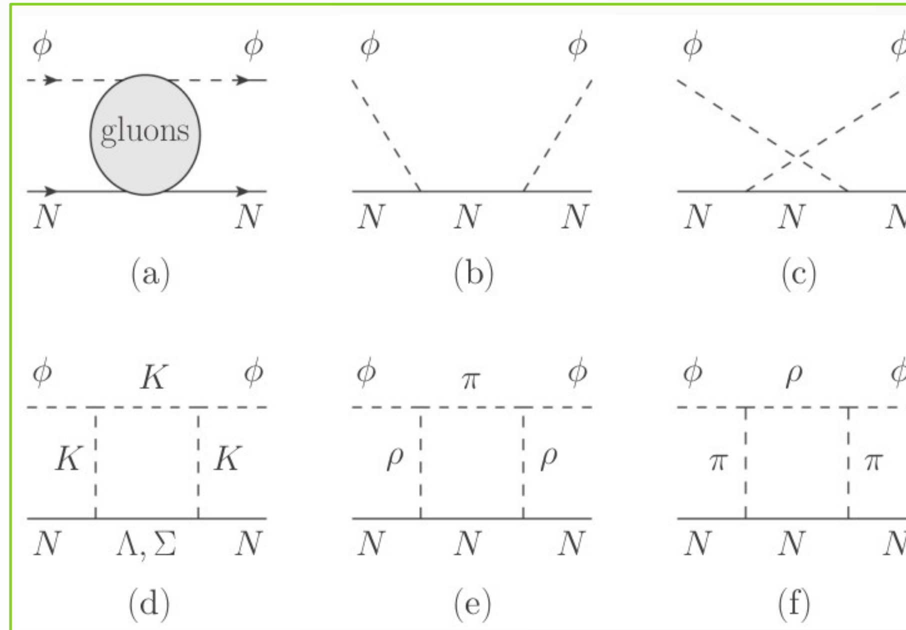

final state interaction (FSI)

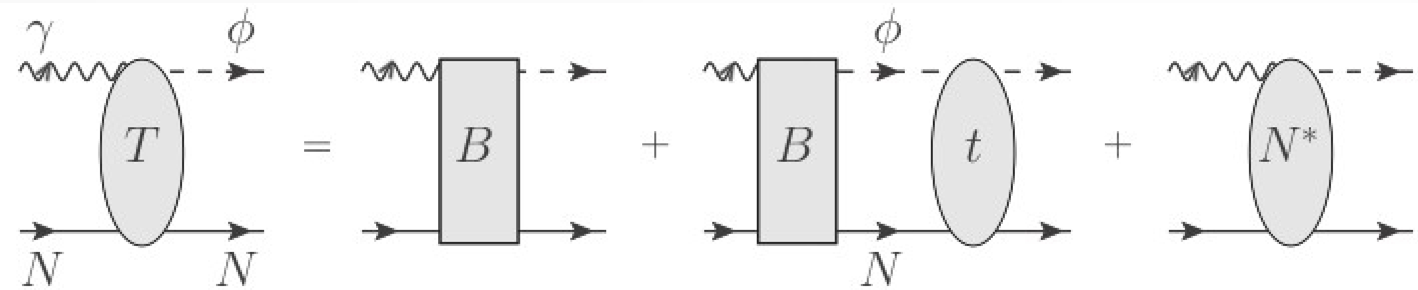

$$T_{\phi N,\gamma N}(E) = B_{\phi N,\gamma N} + T^{\mathrm{FSI}}_{\phi N,\gamma N}(E) + T^{N^*}_{\phi N,\gamma N}(E)$$

$$T^{\mathrm{FSI}}_{\phi N,\gamma N}(E) = t_{\phi N,\phi N}(E) G_{\phi N}(E) B_{\phi N,\gamma N}$$

$$G_{MB}(E) = \frac{|MB\rangle \langle MB|}{E - H_0 + i\epsilon}$$: meson-baryon propagator

$$t_{\phi N,\phi N}(E) = V_{\phi N,\phi N}(E) + V_{\phi N,\phi N} G_{\phi N}(E) t_{\phi N,\phi N}(E)$$

$$V_{\phi N,\phi N}(E) = v^{\mathrm{Gluon}}_{\phi N,\phi N} + v^{\mathrm{Direct}}_{\phi N,\phi N} + \sum_{MB} v_{\phi N,MB} G_{MB}(E) v_{MB,\phi N}$$

(a) (b,c) (d,e,f) MB = (KΛ, KΣ, πN, ρN)

$t_{\phi N,\phi N}(E)$

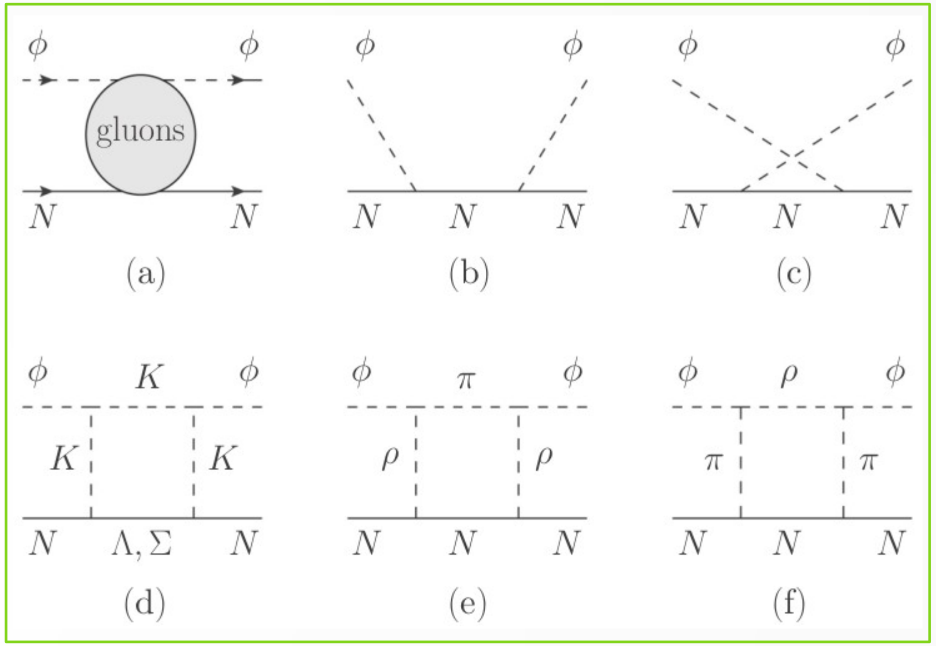

□ To leading order, we obtain these FSI diagrams.

final state interaction (FSI)

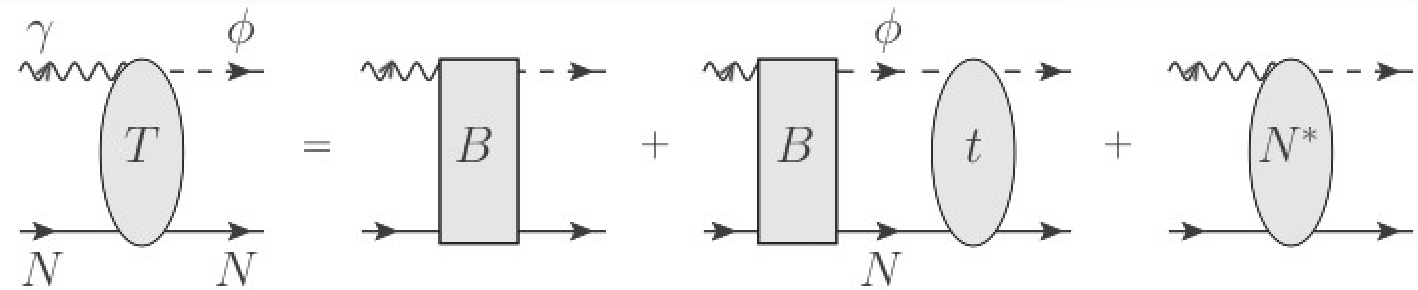

$$T_{\phi N,\gamma N}(E) = B_{\phi N,\gamma N} + T^{\mathrm{FSI}}_{\phi N,\gamma N}(E) + T^{N^*}_{\phi N,\gamma N}(E)$$

$$T^{\mathrm{FSI}}_{\phi N,\gamma N}(E) = t_{\phi N,\phi N}(E) G_{\phi N}(E) B_{\phi N,\gamma N}$$

$$G_{MB}(E) = \frac{|MB\rangle \langle MB|}{E - H_0 + i\epsilon}$$: meson-baryon propagator

$$t_{\phi N,\phi N}(E) = V_{\phi N,\phi N}(E) + V_{\phi N,\phi N} G_{\phi N}(E) t_{\phi N,\phi N}(E)$$

$$V_{\phi N,\phi N} = v^{\mathrm{Gluon}}_{\phi N,\phi N} + v^{\mathrm{Direct}}_{\phi N,\phi N} + \sum_{MB} v_{\phi N,MB} G_{MB}(E) v_{MB,\phi N}$$

(a) (b,c) (d,e,f) MB = (KΛ, KΣ, πN, ρN)

$t_{\phi N,\phi N}(E)$

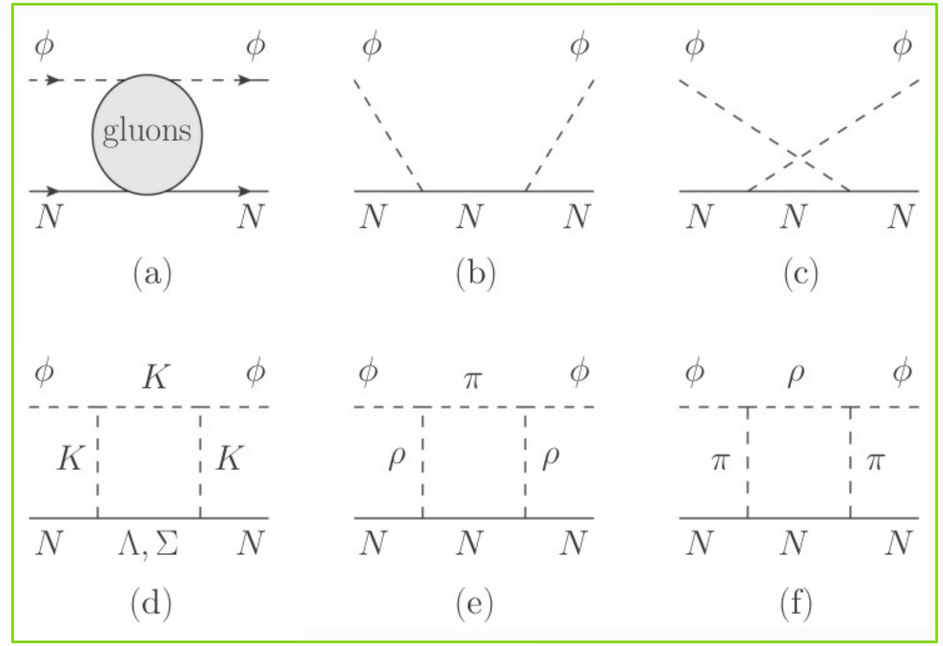

$$\frac{1}{E - H_0 + i\epsilon} = P\frac{1}{E - H_0} - i\pi\delta(E - H_0)$$

□ We consider both parts numerically.

final state interaction (FSI)

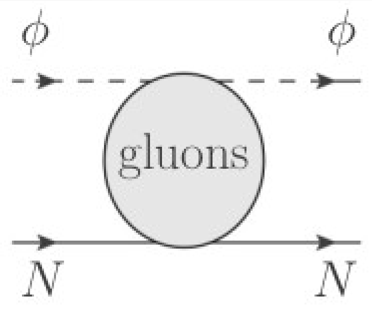

- □ The J/ψ-N potential from the LQCD data
  ~ Yukawa form ($\upsilon_0 = 0.1$, $\alpha = 0.3$ GeV)

  [Kawanai, Sasaki, PRD.82.091501(R) (2010)]

$$\mathcal{V}_{\text{gluon}} = -v_0 \frac{e^{-\alpha r}}{r}$$

- □ which is assumed in our work, φ-N potential
  The best fit was obtained by ($\upsilon_0 = 0.2$, $\alpha = 0.5$ GeV).

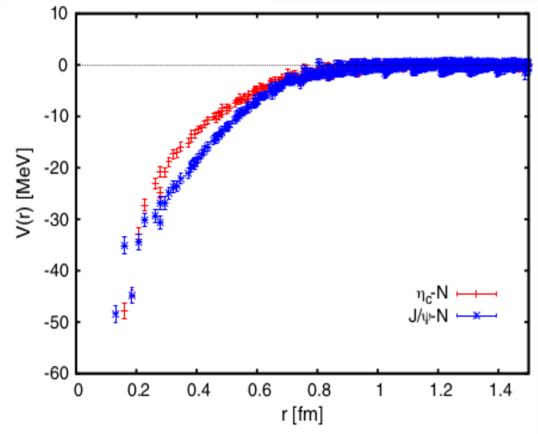

final state interaction (FSI)

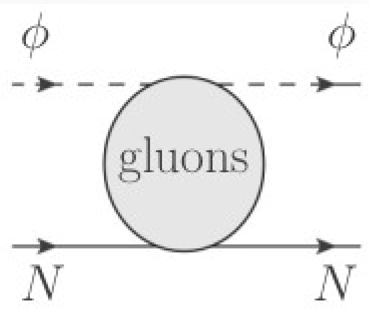

□ The J/ψ-N potential from the LQCD data
~ Yukawa form ($\upsilon_0 = 0.1$, $\alpha = 0.3$ GeV)
[Kawanai, Sasaki, PRD.82.091501(R) (2010)]

$$\mathcal{V}_{\text{gluon}} = -\upsilon_0 \frac{e^{-\alpha r}}{r}$$

□ which is assumed in our work, φ-N potential
The best fit was obtained by ($\upsilon_0 = 0.2$, $\alpha = 0.5$ GeV).

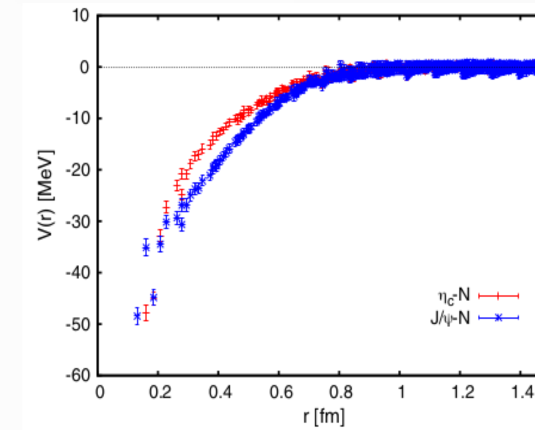

□ The potential is obtained by taking the nonrelativistic limit of the scalar-meson exchange amplitude calculated from the Lagrangian:

$$\mathscr{L}_\sigma = V_0(\bar{\psi}_N \psi_N \Phi_\sigma + \phi^\mu \phi_\mu \Phi_\sigma)$$

Φ_σ is a scalar field with mass α ($V_0 = -8\upsilon_0 \pi M_\varphi$).

□ $$\mathcal{V}_{\text{gluon}}(k\lambda_\phi, pm_s; k'\lambda'_\phi, p'm'_s) = \frac{V_0}{(p-p')^2 - \alpha^2}[\bar{u}_N(p, m_s)u_N(p', m'_s)][\epsilon^*_\mu(k, \lambda_\phi)\epsilon^\mu(k', \lambda'_\phi)]$$

final state interaction (FSI)

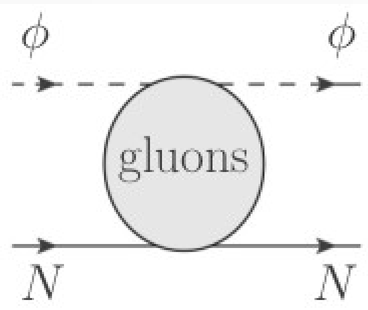

□ The J/ψ-N potential from the LQCD data
~ Yukawa form (υ_0 = 0.1, α = 0.3 GeV)
[Kawanai, Sasaki, PRD.82.091501(R) (2010)]

$$\mathcal{V}_{\rm gluon} = -\upsilon_0 \frac{e^{-\alpha r}}{r}$$

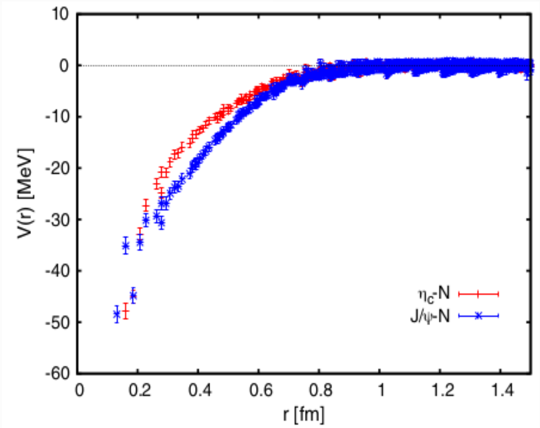

□ which is assumed in our work, φ-N potential
The best fit was obtained by (υ_0 = 0.2, α = 0.5 GeV).

□ The φ-N potential from the LQCD [Lyu, PRD.106.074507 (2022)]

Attractive N-ϕ Interaction and Two-Pion Tail from Lattice QCD near Physical Point

Yan Lyu,[1,2,*] Takumi Doi,[2,†] Tetsuo Hatsuda,[2,‡] Yoichi Ikeda,[3,§]
Jie Meng,[1,4,¶] Kenji Sasaki,[3,**] and Takuya Sugiura[2,††]

□ The simple fitting functions such as
"the Yukawa form" and "the van der Waals form ~ $1/r^k$ with k=6(7)"
cannot reproduce the lattice data.
> We need to update our results based on the LQCD data.

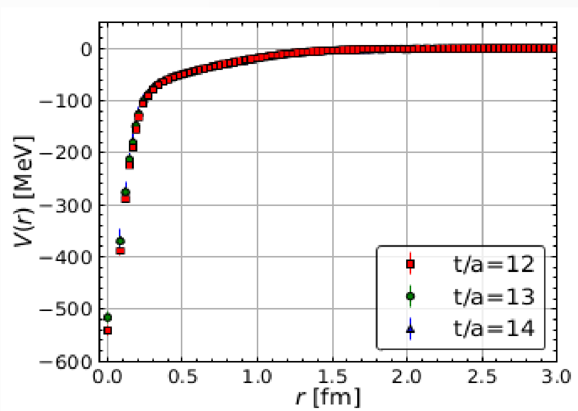

FIG. 1. (Color online). The N-ϕ potential $V(r)$ in the $^4S_{3/2}$ channel as a function of separation r at Euclidean time t/a = 12 (red squares), 13 (green circles) and 14 (blue triangles).

Born term

total cross section [γ p → φ p]

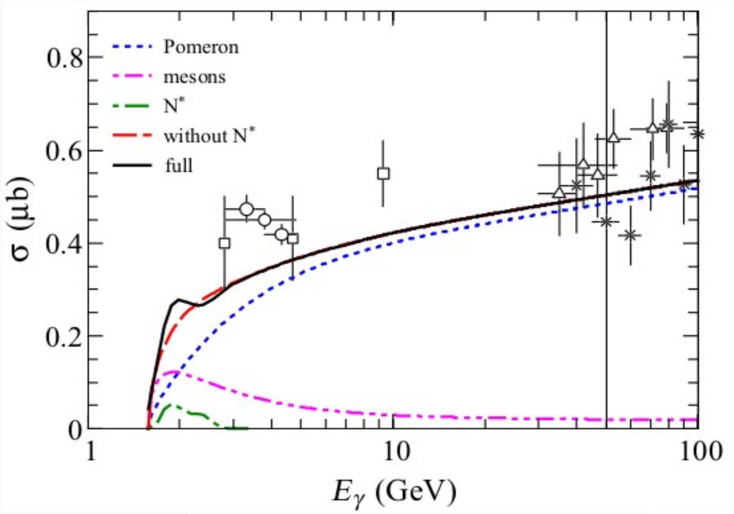

Born term

total cross section [γ p → φ p]

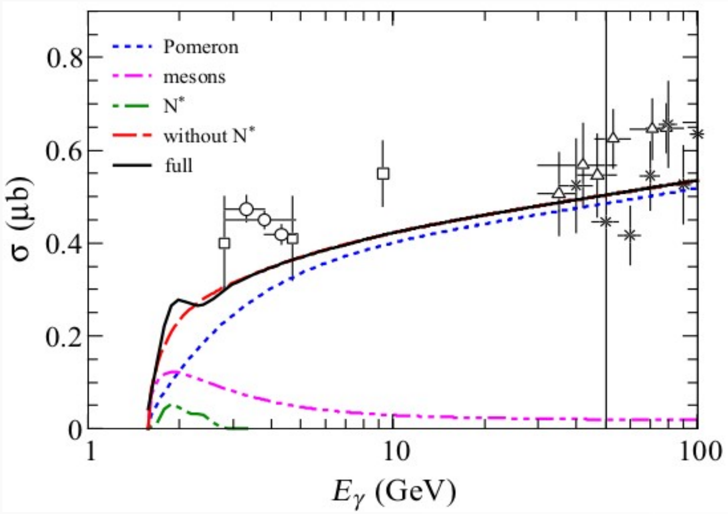

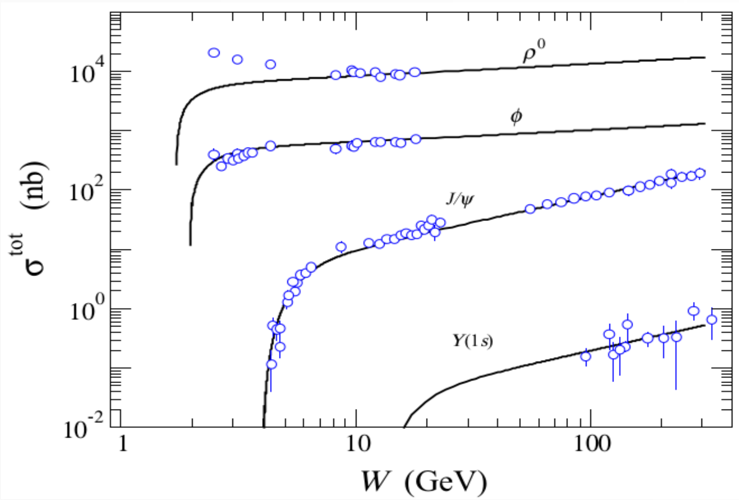

γ p →
ρ^0
ω
φ
J/ψ
ϒ(1s)

- Our Pomeron model describes the high energy regions quite well.

Born term total cross section [γ p → φ p] with FSI

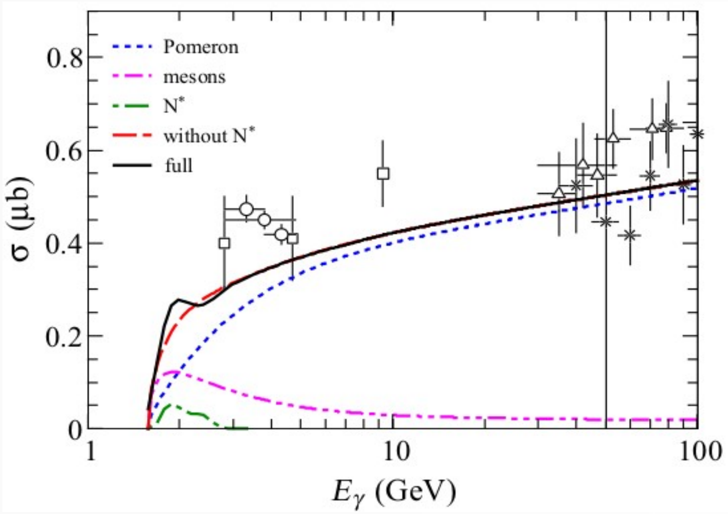

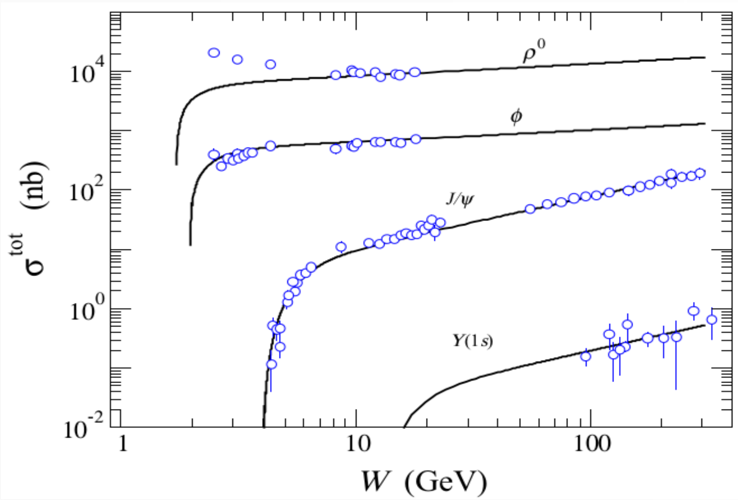

γ p →
ρ^0
ω
φ
J/ψ
Υ(1s)

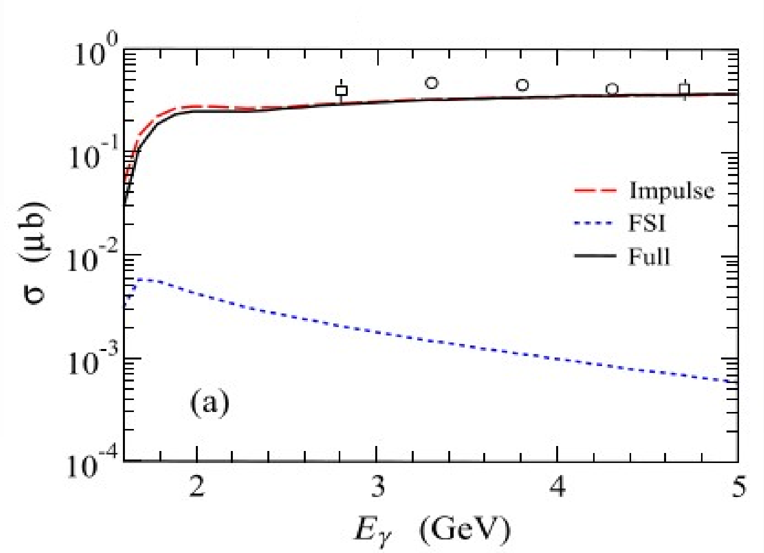

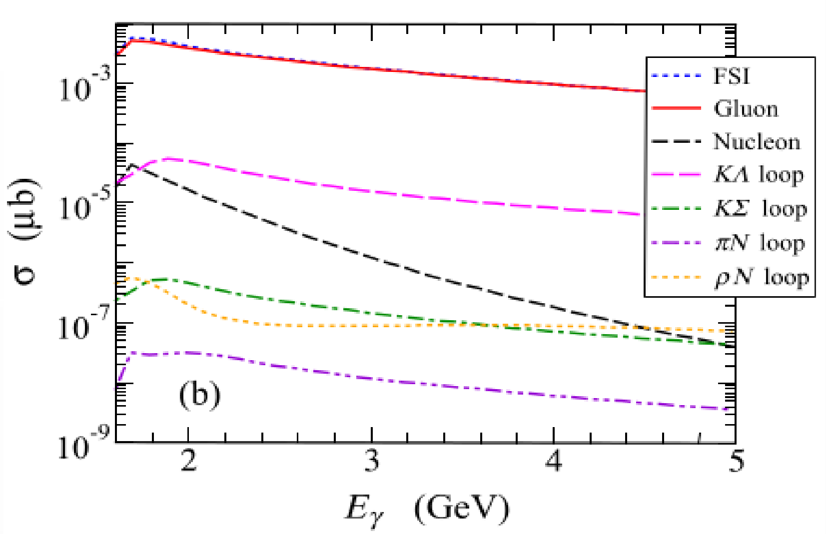

□ Our Pomeron model describes the high energy regions quite well.

□ The contributions of the FSI terms are almost very small.

differential cross sections
[γ p → φ p]

Born term

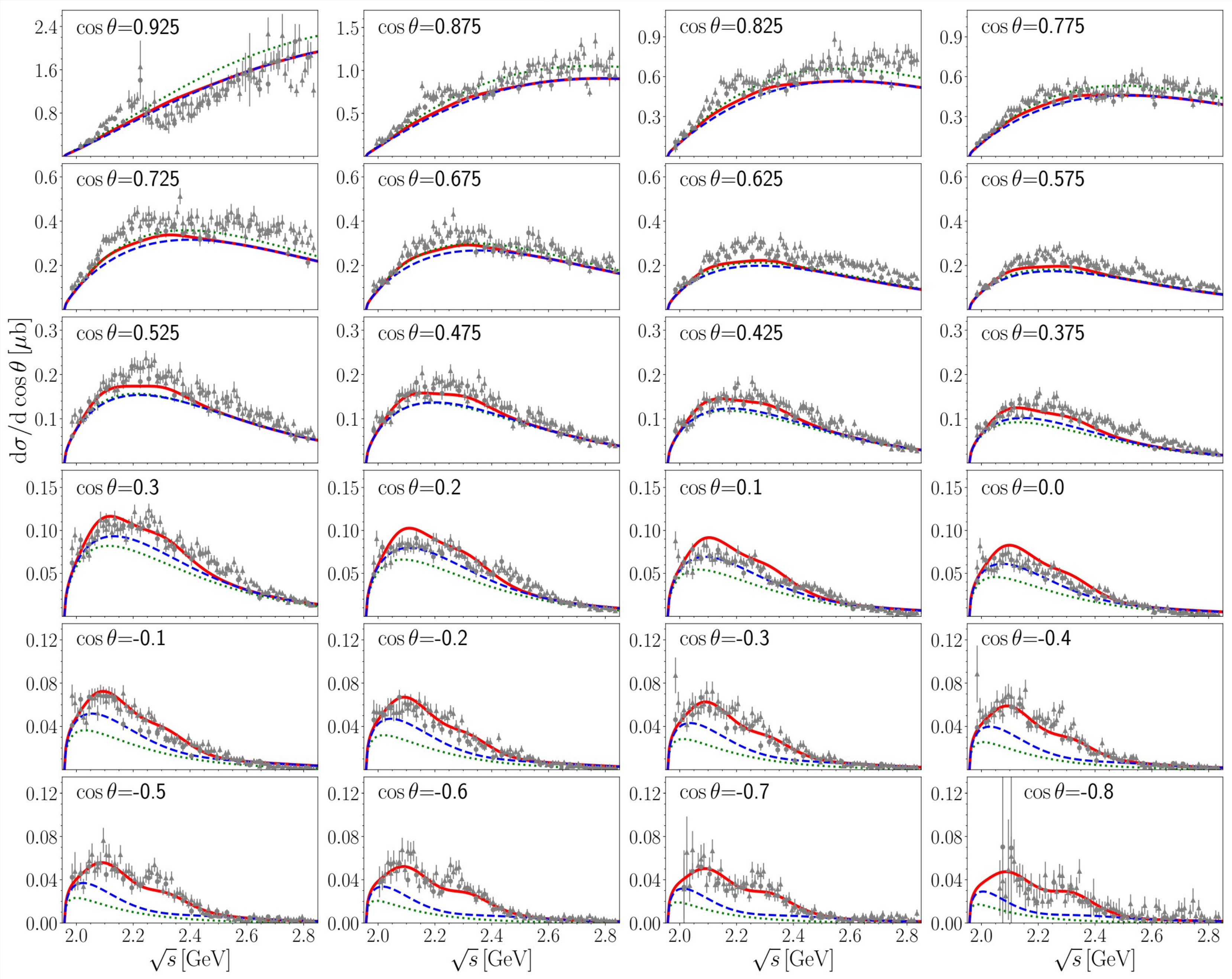

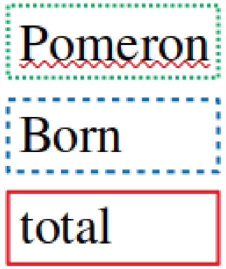

[Exp: Dey (CLAS), PRC.89. 055208 (2014)]

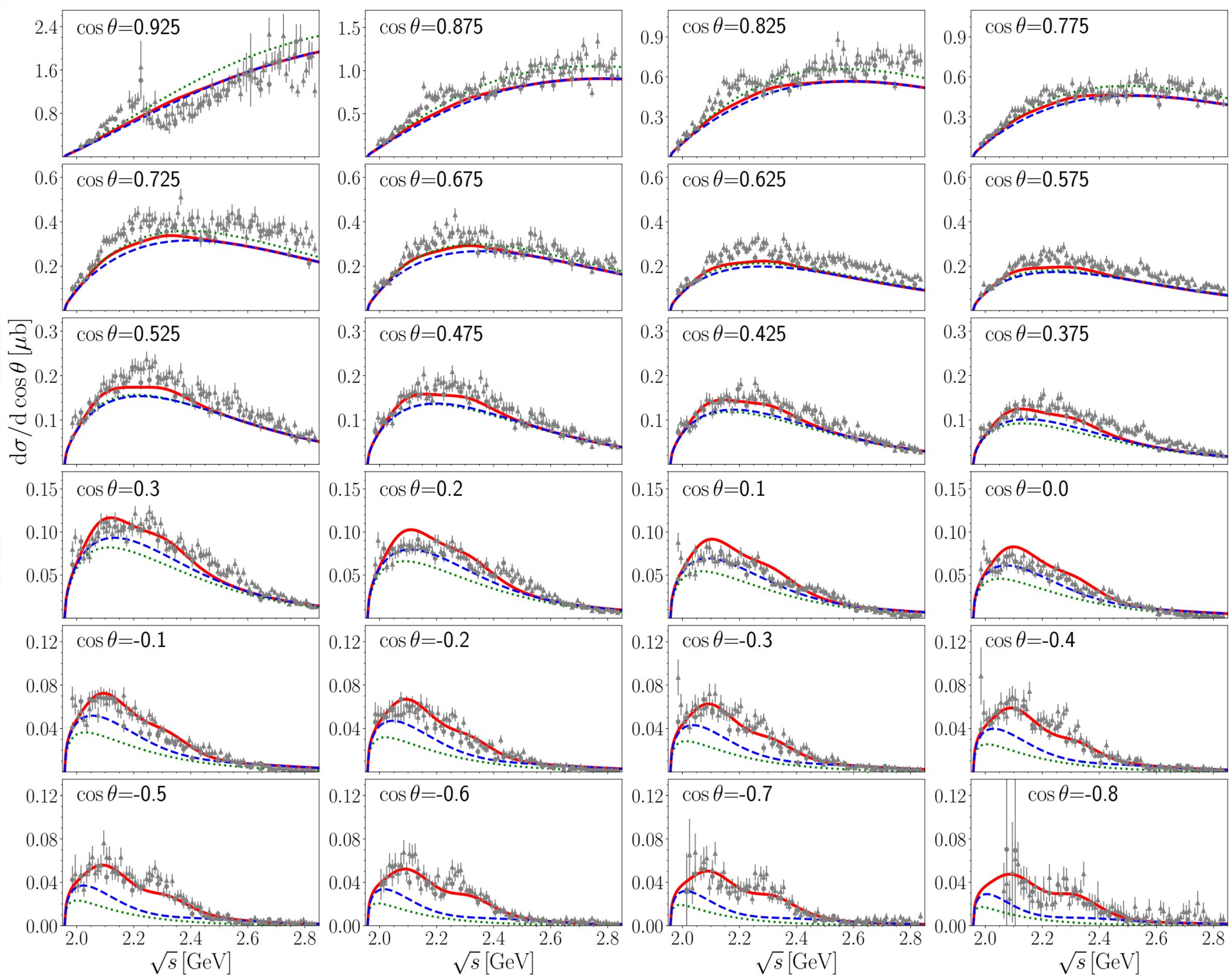

differential cross sections

[$\gamma\, p \to \varphi\, p$]

- □ The strong peak at $\sqrt{s} \simeq 2.2$ GeV persists only in cosθ = 0.925 & vanishes around cosθ = 0.8.
- □ The backward peaks at $\sqrt{s} \simeq 2.1$ & 2.3 GeV are due to two N^*'s although the magnitudes are far more suppressed.

Pomeron

Born

total

[Exp: Dey (CLAS), PRC.89. 055208 (2014)]

[Ryu, PTEP.2014.023D03 (2014)]

$$\mathcal{M}_{\gamma N\to\phi N}(p,p';s) = \mathcal{M}^{\mathrm{Born}}_{\gamma N\to\phi N}(p,p';s) + \sum_i \int \mathrm{d}^3q \frac{E_{M_i}+E_{B_i}}{(2\pi)^3 2E_{M_i}E_{B_i}} \mathcal{M}_{\gamma N\to M_iB_i}(p,q;s) \frac{1}{s^2-(E_{M_i}+E_{B_i})^2+i\varepsilon} \mathcal{M}_{M_iB_i\to\phi N}(q,p';s), \quad (1)$$

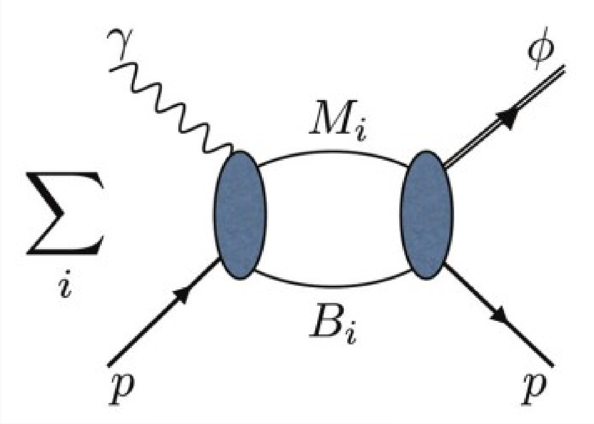

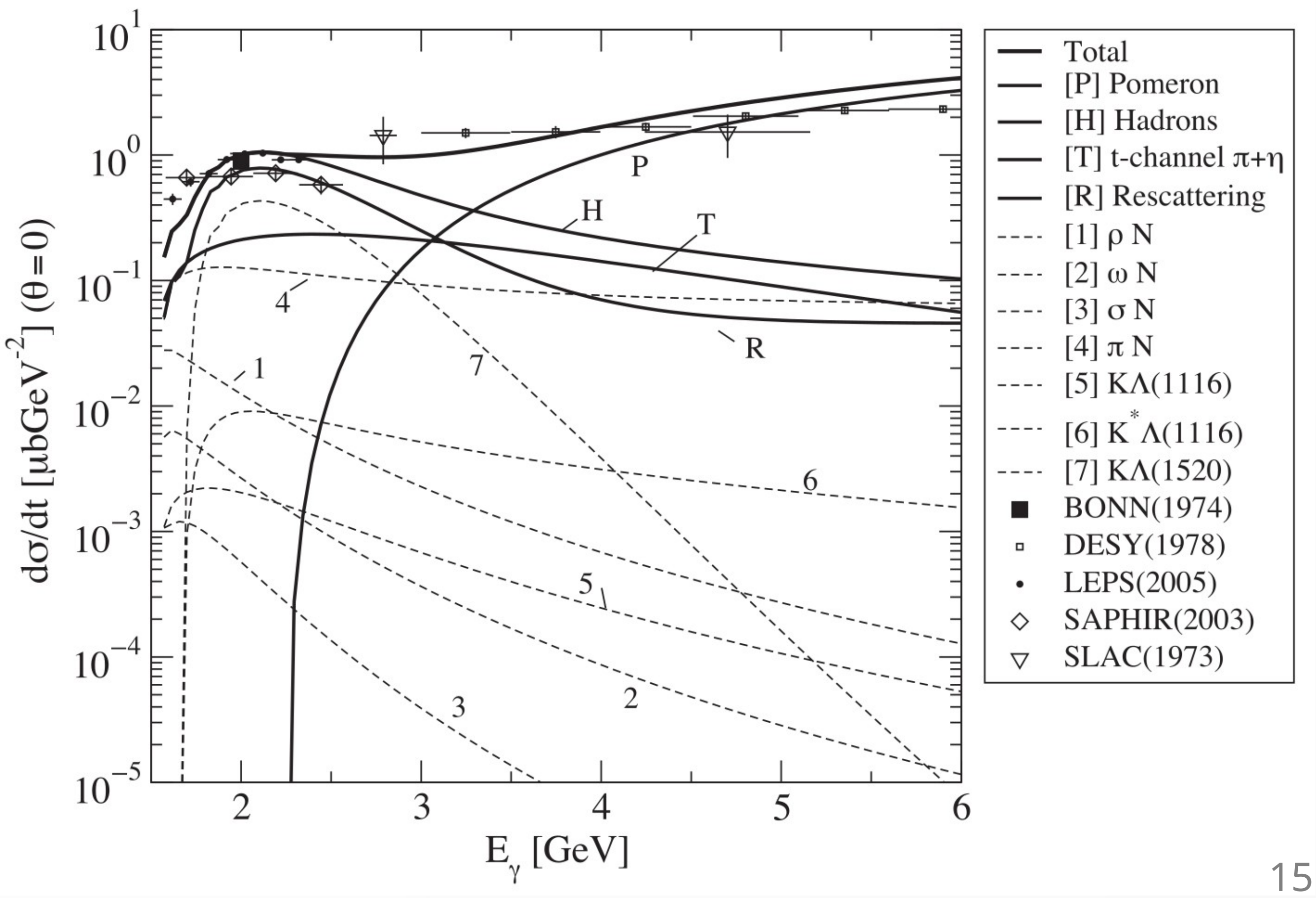

□ They considered only
the imaginary part of the propagator.
The real part should be considered.

❑ We employ a distorted-wave impulse approximation.

$$F_c(q^2) = F_N(q^2)F_T(q^2 = t)$$

F_c (F_N) : nuclear (nucleon) charge FF

□ Including the FSI term, we can write DCS for spin J=0 nuclei:

$$\frac{d\sigma}{d\Omega_{\rm Lab}} = \frac{(2\pi)^4|\mathbf{k}|^2E_V(\mathbf{k})E_A(\mathbf{q}-\mathbf{k})}{|E_A(\mathbf{q}-\mathbf{k})|\mathbf{k}| + E_V(\mathbf{k})(|\mathbf{k}| - |\mathbf{q}|\cos\theta_{\rm Lab})|}|AF_T(t)\bar{t}(\mathbf{k},\mathbf{q}) + T^{\rm FSI}(\mathbf{k},\mathbf{q},E)|^2$$

$\gamma\ {}^4He \to \varphi\ {}^4He$ $\gamma\ p \to \varphi\ p$

$$T(E) = T^{\rm IMP}(E) + T^{\rm FSI}(E)$$

$$T^{\rm IMP} = \sum_{i=1,A}\left[B_{\phi N_i,\gamma N_i} + T^{N^*}_{\phi N_i,\gamma N_i}\right]$$

❑ We employ a distorted-wave impulse approximation.

□ Including the FSI term, we can write DCS for spin J=0 nuclei:

$$F_c(q^2) = F_N(q^2) F_T(q^2 = t)$$

F_c (F_N) : nuclear (nucleon) charge FF

$$\frac{d\sigma}{d\Omega_{\rm Lab}} = \frac{(2\pi)^4 |\mathbf{k}|^2 E_V(\mathbf{k}) E_A(\mathbf{q}-\mathbf{k})}{|E_A(\mathbf{q}-\mathbf{k})|\mathbf{k}| + E_V(\mathbf{k})(|\mathbf{k}| - |\mathbf{q}|\cos\theta_{\rm Lab})|} |A F_T(t) \bar{t}(\mathbf{k},\mathbf{q}) + T^{\rm FSI}(\mathbf{k},\mathbf{q},E)|^2$$

γ ^{4}He → φ ^{4}He   γ p → φ p

$$T(E) = T^{\rm IMP}(E) + T^{\rm FSI}(E)$$

$$T^{\rm IMP} = \sum_{i=1,A} [B_{\phi N_i,\gamma N_i} + T^{N^*}_{\phi N_i,\gamma N_i}]$$

$$T^{FSI}(\mathbf{k},\mathbf{q},E) = \int d\mathbf{k}' T_{\phi A,\phi A}(\mathbf{k},\mathbf{k}',E) \frac{A F(t') \bar{t}(\mathbf{k}',\mathbf{q})}{E - E_V(\mathbf{k}') - E_A(\mathbf{q}-\mathbf{k}') + i\epsilon}$$

$$T^{\rm FSI}(E) = T_{\phi A,\phi A}(E) \frac{1}{E - H_0} T^{\rm IMP}$$

□ $T^{\rm IMP}$: the term that φ meson is produced from a single nucleon in the nucleus

□ $T^{\rm FSI}$: the effect due to the scattering of the outgoing φ with the recoiled nucleus

$$T_{\phi A,\phi A}(\boldsymbol{\kappa},\boldsymbol{\kappa}',E) = U_{\phi A,\phi A}(\boldsymbol{\kappa},\boldsymbol{\kappa}',E) + \int d\boldsymbol{\kappa}'' U_{\phi A,\phi A}(\boldsymbol{\kappa},\boldsymbol{\kappa}'',E) \frac{1}{E - E_V(\boldsymbol{\kappa}'') - E_A(\boldsymbol{\kappa}'') + i\epsilon} T_{\phi A,\phi A}(\boldsymbol{\kappa}'',\boldsymbol{\kappa}',E) \quad \text{(in c.m.)}$$

□ Within multiple-scattering theory, φA potential is expressed in terms of φN scattering amplitude.

$$U_{\phi A,\phi A}(E) = \sum_{i=1,A} t_{\phi N_i,\phi N_i}(\omega)$$

❑ We employ a distorted-wave impulse approximation.

□ Including the FSI term, we can write DCS for spin J=0 nuclei:

$$F_c(q^2) = F_N(q^2)F_T(q^2 = t)$$

F_c (F_N) : nuclear (nucleon) charge FF

$$\frac{d\sigma}{d\Omega_{\rm Lab}} = \frac{(2\pi)^4|\mathbf{k}|^2 E_V(\mathbf{k})E_A(\mathbf{q}-\mathbf{k})}{|E_A(\mathbf{q}-\mathbf{k})|\mathbf{k}| + E_V(\mathbf{k})(|\mathbf{k}| - |\mathbf{q}|\cos\theta_{\rm Lab})|}\,|AF_T(t)\bar{t}(\mathbf{k},\mathbf{q}) + T^{\rm FSI}(\mathbf{k},\mathbf{q},E)|^2$$

γ ^{4}He → φ ^{4}He γ p → φ p

$$T(E) = T^{\rm IMP}(E) + T^{\rm FSI}(E)$$

$$T^{\rm IMP} = \sum_{i=1,A}[B_{\phi N_i,\gamma N_i} + T^{N^*}_{\phi N_i,\gamma N_i}]$$

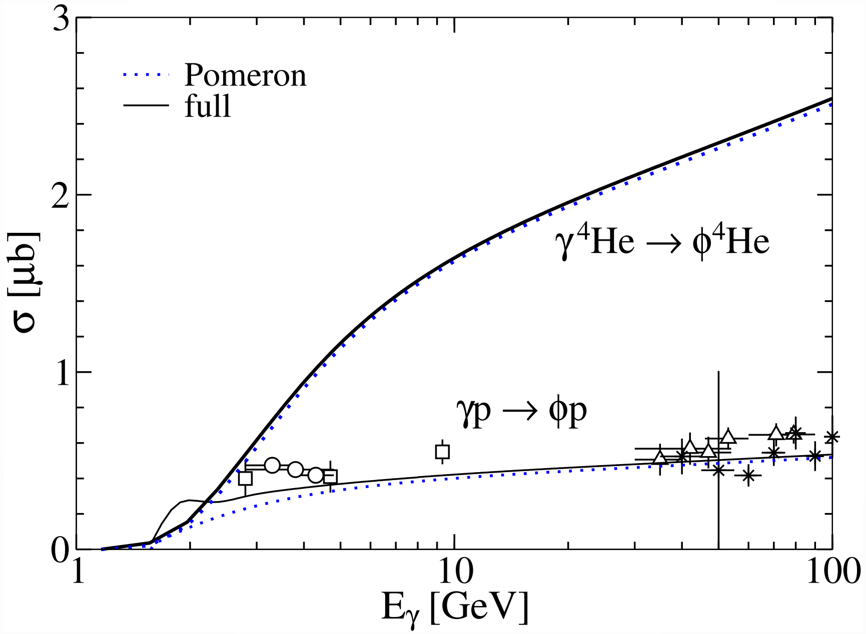

□ The total cross section for φ^{4}He production is about 4 times larger than φN production.

❑ We employ a distorted-wave impulse approximation.

$$F_c(q^2) = F_N(q^2)F_T(q^2 = t)$$

Fc (FN) : nuclear (nucleon) charge FF

□ Including the FSI term, we can write DCS for spin J=0 nuclei:

$$\frac{d\sigma}{d\Omega_{\rm Lab}} = \frac{(2\pi)^4|\mathbf{k}|^2 E_V(\mathbf{k})E_A(\mathbf{q}-\mathbf{k})}{|E_A(\mathbf{q}-\mathbf{k})|\mathbf{k}| + E_V(\mathbf{k})(|\mathbf{k}| - |\mathbf{q}|\cos\theta_{\rm Lab})|}\,|AF_T(t)\bar{t}(\mathbf{k},\mathbf{q}) + T^{\rm FSI}(\mathbf{k},\mathbf{q},E)|^2$$

$$T(E) = T^{\rm IMP}(E) + T^{\rm FSI}(E)$$

$$T^{\rm IMP} = \sum_{i=1,A}\left[B_{\phi N_i,\gamma N_i} + T^{N^*}_{\phi N_i,\gamma N_i}\right]$$

γ ^{4}He → φ ^{4}He   γ p → φ p

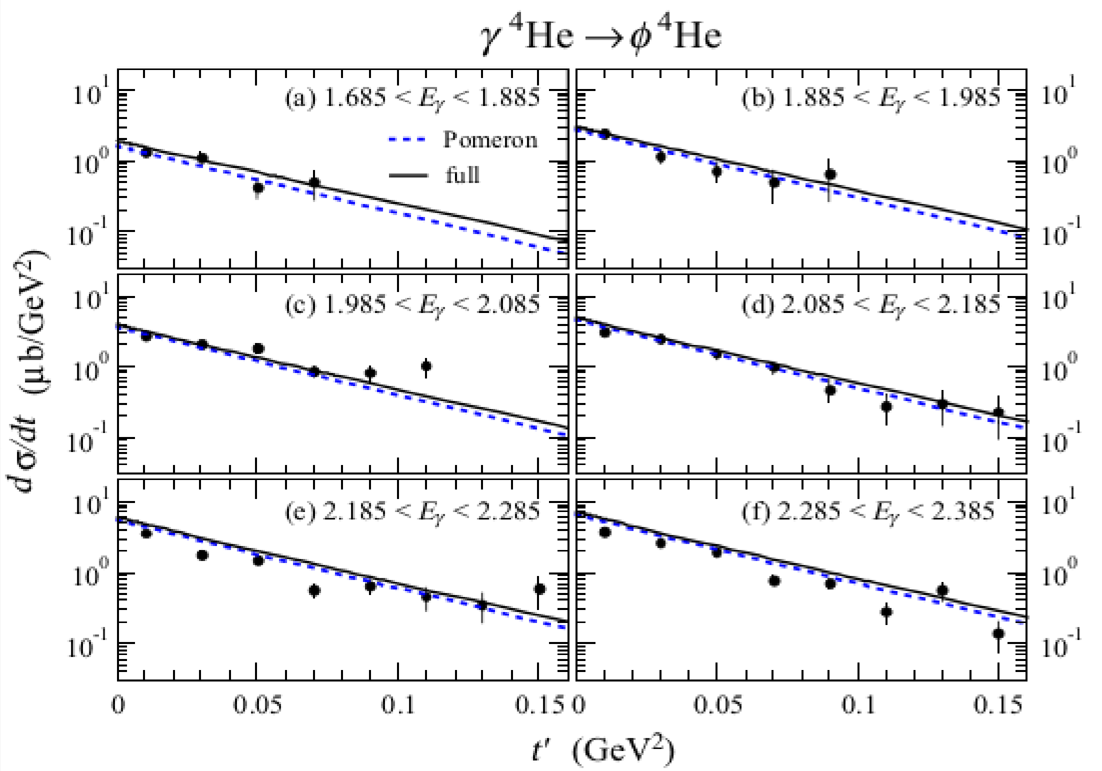

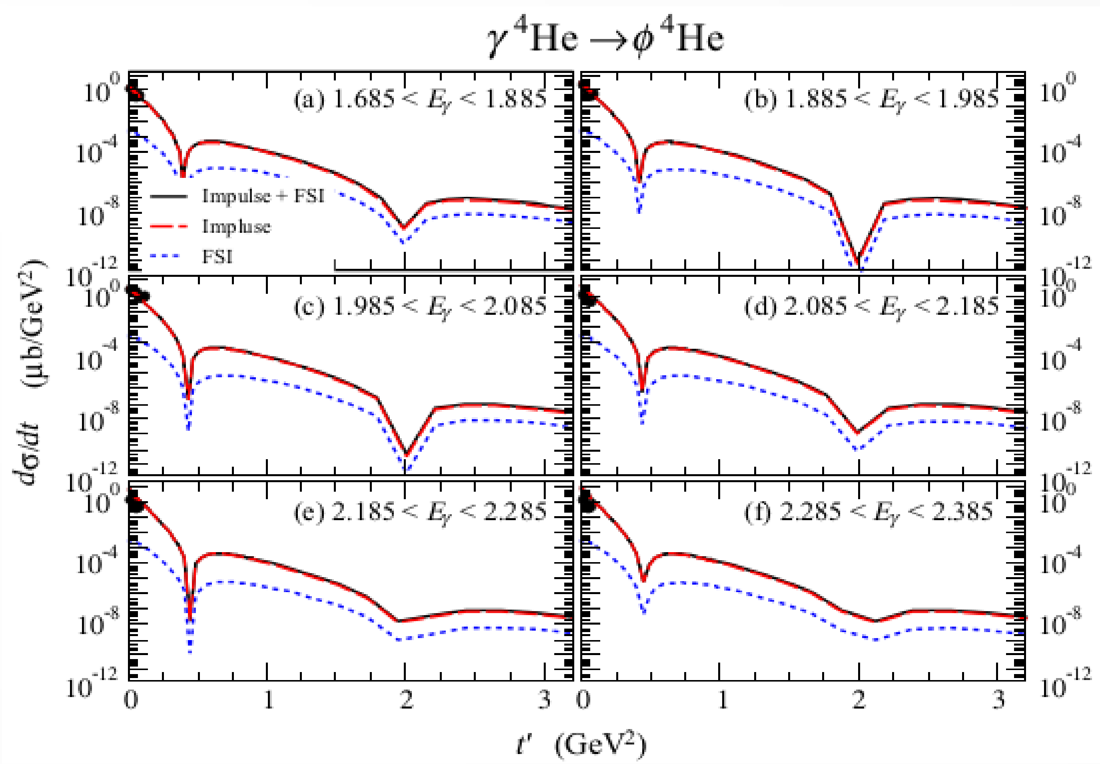

□ The FSI contributions are relatively suppressed by factors of $10^1 - 10^3$.

$\gamma\ p \to \varphi\ p$

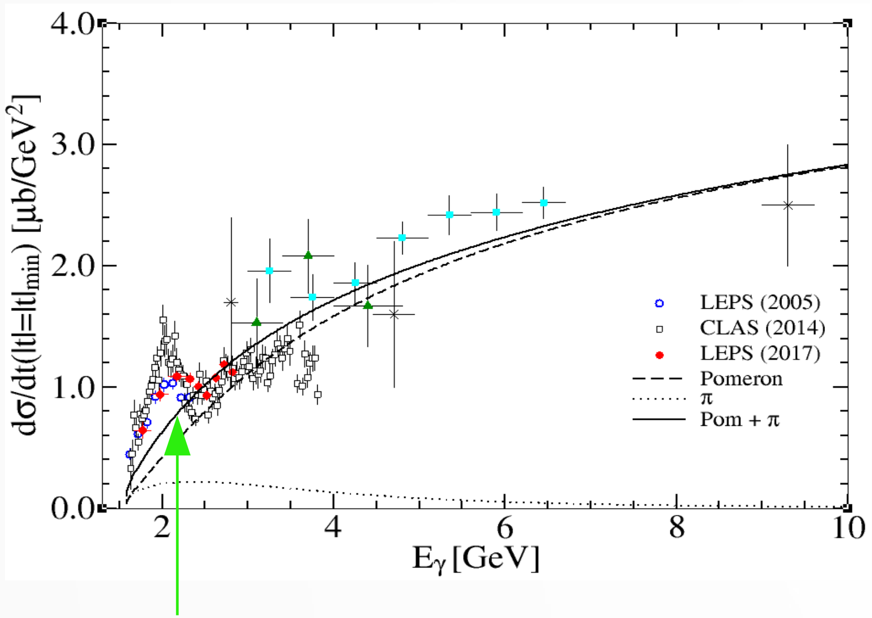

- is not due to the N^* contribution.
- may arise from another mechanism.

$\gamma\ ^4He \to \varphi\ ^4He$

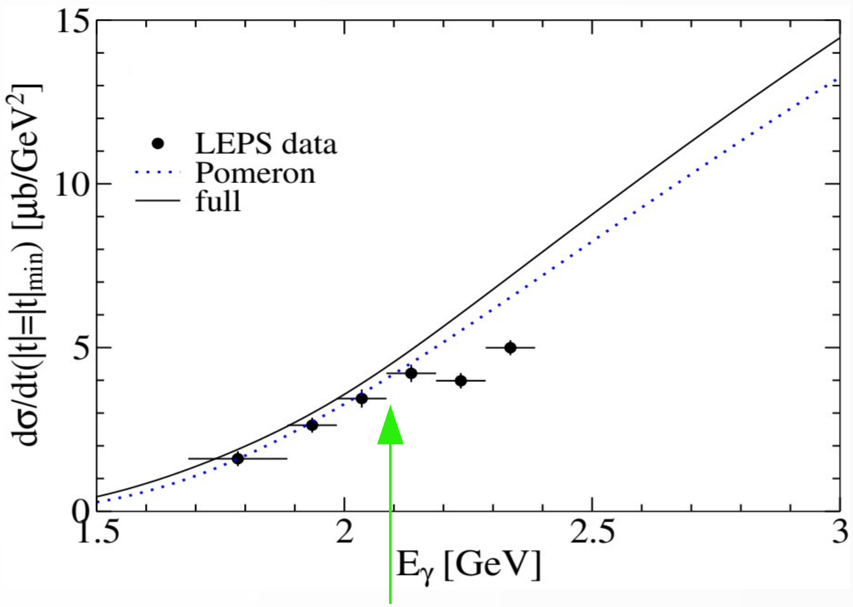

[Exp: Hiraiwa (LEPS), PRC.035208.5 (2017)]

□ The peak position is similar to each other.
Any relation between them?

2. $\gamma\, p \rightarrow J/\psi\, p$, $\gamma\, {}^4He \rightarrow J/\psi\, {}^4He$

$\gamma\, d \rightarrow J/\psi\, d$

[S.Sakinah, T.-S.H.Lee, H.M.Choi, PRC.109.065204 (2024)]

□ They obtain the phenomenological J/ψ potentials, $V^{J/\psi N \to J/\psi N}$, with no VMD assumption by taking the $c\bar{c}$ structure of J/ψ into account to define the model Hamiltonian: $H = H_0 + \Gamma_{\gamma,c\bar{c}} + v_{c\bar{c}} + v_{cN}$

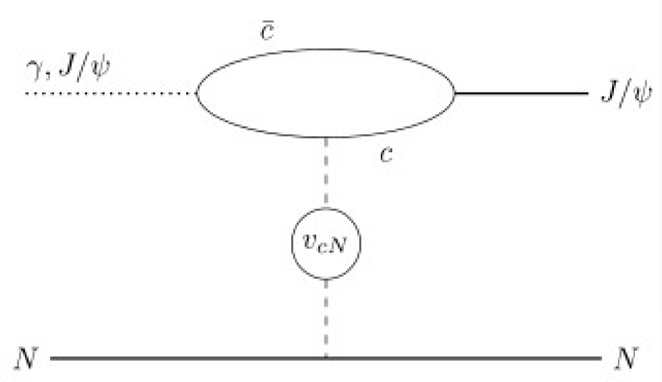

□ It is assumed that the interactions between the $c\bar{c}$ quarks in J/ψ and the nucleon can be defined by a phenomenological quark-N potential v_{cN}.

□ The $\gamma N \to J/\psi N$ amplitude, $B^{\gamma N \to J/\psi N}$, and $J/\psi N \to J/\psi N$ potential, $V^{J/\psi N \to J/\psi N}$, are defined by the $c\bar{c}$-loop mechanisms.

[S.Sakinah, T.-S.H.Lee, H.M.Choi, PRC.109.065204 (2024)]

□ They obtain the phenomenological J/ψ potentials, $V^{J/\psi N \to J/\psi N}$, with no VMD assumption by taking the $c\bar{c}$ structure of J/ψ into account to define the model Hamiltonian: $H = H_0 + \Gamma_{\gamma, c\bar{c}} + v_{c\bar{c}} + v_{cN}$

□ It is assumed that the interactions between the $c\bar{c}$ quarks in J/ψ and the nucleon can be defined by a phenomenological quark-N potential v_{cN}.

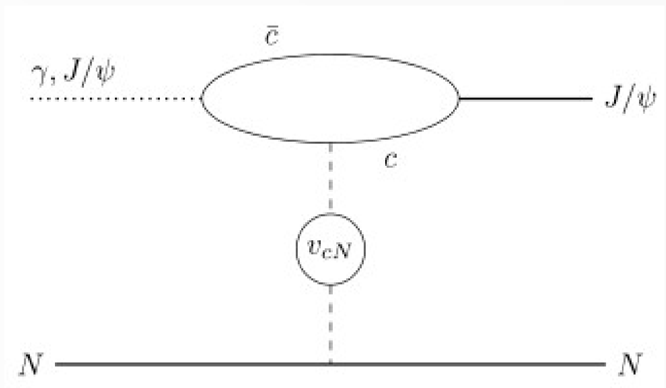

□ The $\gamma N \to J/\psi N$ amplitude, $B^{\gamma N \to J/\psi N}$, and $J/\psi N \to J/\psi N$ potential, $V^{J/\psi N \to J/\psi N}$, are defined by the $c\bar{c}$-loop mechanisms.

□ The unitary condition requires the J/ψ-N FSI effects must be included.

$$T_{total}^{\gamma N \to J/\psi N} = T_D^{\gamma N \to J/\psi N} + T_{Pom}^{\gamma N \to J/\psi N}$$
$$= (B^{\gamma N \to J/\psi N} + T_{fsi}^{\gamma N \to J/\psi N}) + T_{Pom}^{\gamma N \to J/\psi N}$$

with $T_{fsi}^{\gamma N \to J/\psi N} = T^{J/\psi N \to J/\psi N} \frac{1}{W - H_0 + i\epsilon} B^{\gamma N \to J/\psi N}$

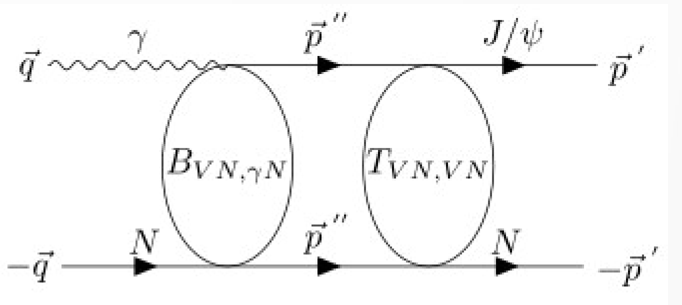

□ $T^{J/\psi N \to J/\psi N}$ scattering amplitude is calculated from $V^{J/\psi N \to J/\psi N}$ potential, by solving the Lippman-Schwinger equation :

$$T^{J/\psi N \to J/\psi N} = V^{J/\psi N \to J/\psi N} + V^{J/\psi N \to J/\psi N} G^{J/\psi N \to J/\psi N} T^{J/\psi N \to J/\psi N}$$

[S.Sakinah, T.-S.H.Lee, H.M.Choi, PRC.109.065204 (2024)]

□ It is assumed that the VN potential can be constructed by the Folding model using the quark-N interaction v_{cN} and the wave function $\varphi_{J/\psi}$:

$$V_{VN,VN} = \langle \phi_V , N | \sum_c v_{cN} | \phi_V , N \rangle$$

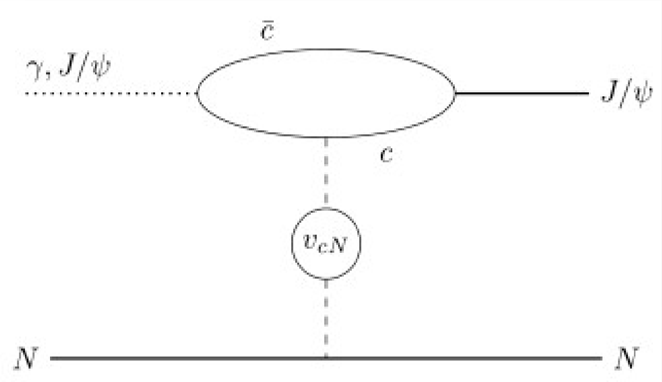

□ The wave function and v_{cN} potential are also used to construct the amplitude:

$$B_{VN,\gamma N}(W) = \langle \phi_V , N | \left[\sum_c v_{cN} \frac{|c\bar{c}\rangle \langle c\bar{c}|}{E_{c\bar{c}} - H_0} \Gamma_{\gamma,c\bar{c}} \right] |\gamma, N\rangle$$

> $T_D^{\gamma N \to J/\psi N}$ is completely determined by $v_{cN}(r)$.

[S.Sakinah, T.-S.H.Lee, H.M.Choi, PRC.109.065204 (2024)]

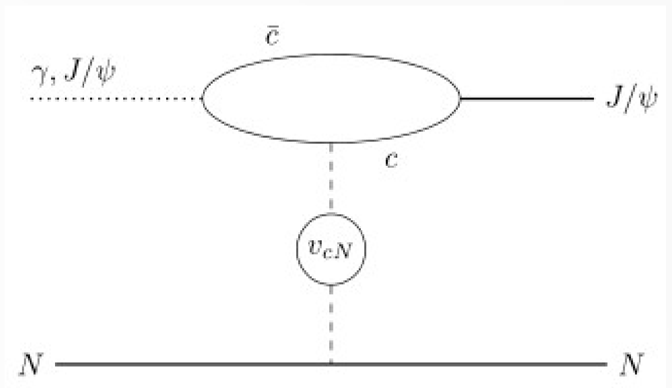

□ It is assumed that the VN potential can be constructed by the Folding model using the quark-N interaction v_{cN} and the wave function $\varphi_{J/\psi}$:

$$V_{VN,VN} = \langle \phi_V , N | \sum_c v_{cN} | \phi_V , N \rangle$$

□ The wave function and v_{cN} potential are also used to construct the amplitude:

$$B_{VN,\gamma N}(W) = \langle \phi_V , N | \left[\sum_c v_{cN} \frac{|c\bar{c}\rangle \langle c\bar{c}|}{E_{c\bar{c}} - H_0} \Gamma_{\gamma, c\bar{c}} \right] | \gamma, N \rangle$$

> $T_D^{\gamma N \to J/\psi N}$ is completely determined by $v_{cN}(r)$.

□ To establish correspondence with the LQCD calculations, $v_{cN}(r)$ is chosen such that the predicted $V_{J/\psi N}(r)$ at large distances exhibits the Yukawa potential form :

$$v_{cN}(r) = \alpha \left(\frac{-\mu r}{r} - c_s \frac{e^{-\mu_1 r}}{r} \right)$$

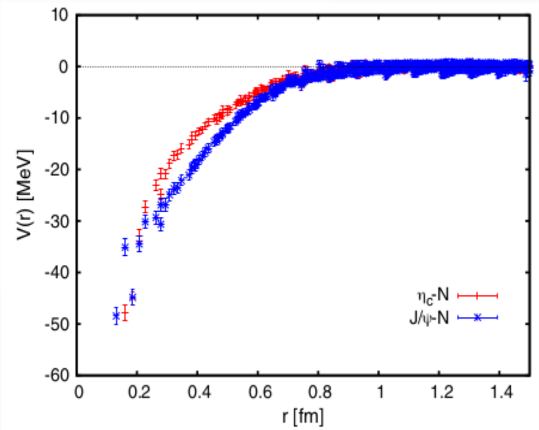

□ 1Y model : α = -0.067, μ = 0.3 GeV, c_s = 0

2Y model : α = -0.145, μ = 0.3 GeV, c_s = 1, $\mu_1 = 5\mu$

[Kawanai, PRD.82.091501(R) (2011)]

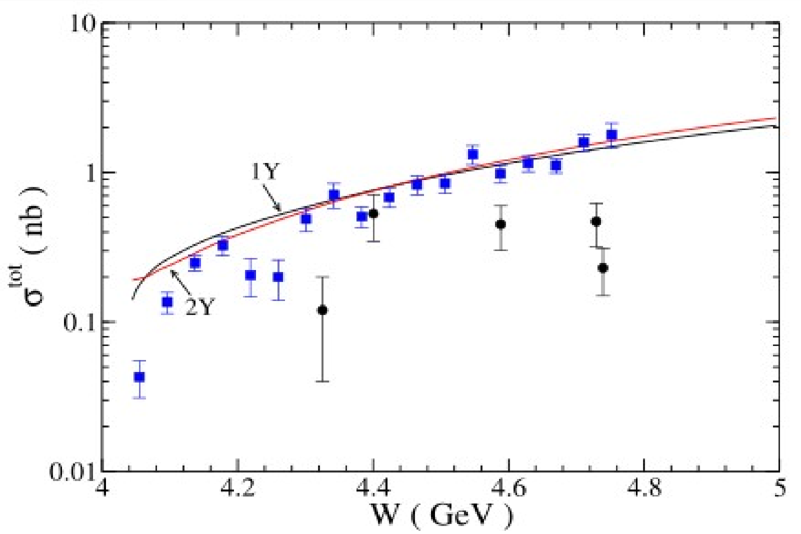

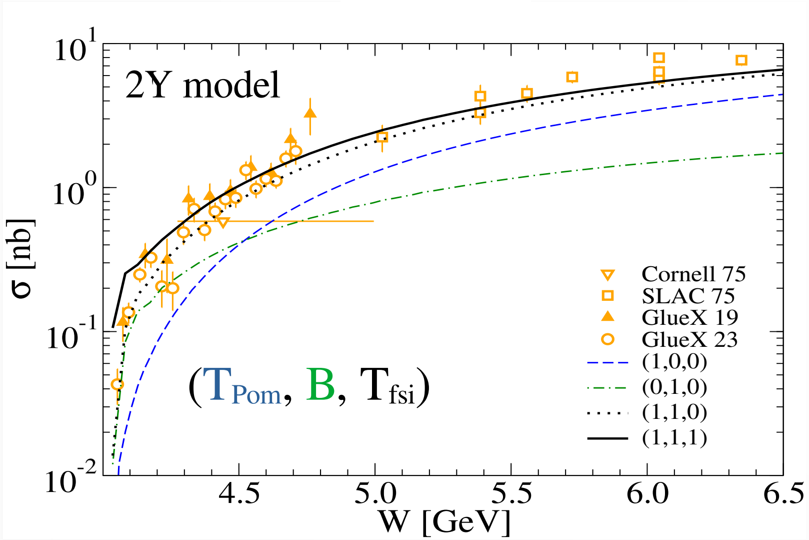

2Y model

□ DL Pomeron exchange alone is not sufficient for describing the diff. cross section data.

□ Together with the determined $v_{cN}(r)$ and wave function $\varphi_{J/\psi}$ generated from CQM, B model, the diff. cross section data could be well reproduced at low energies.

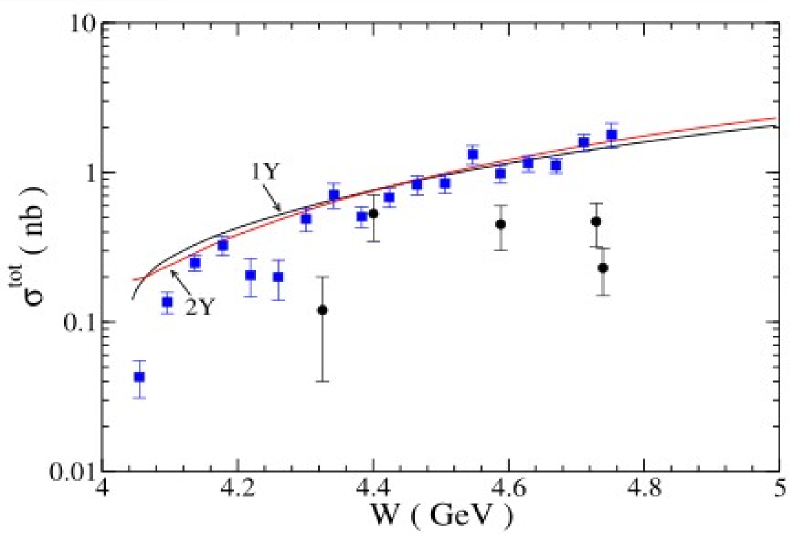

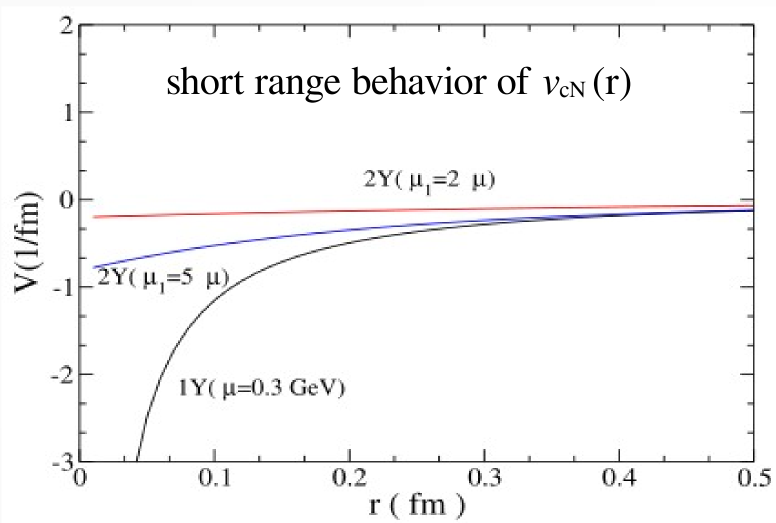

1Y & 2Y models

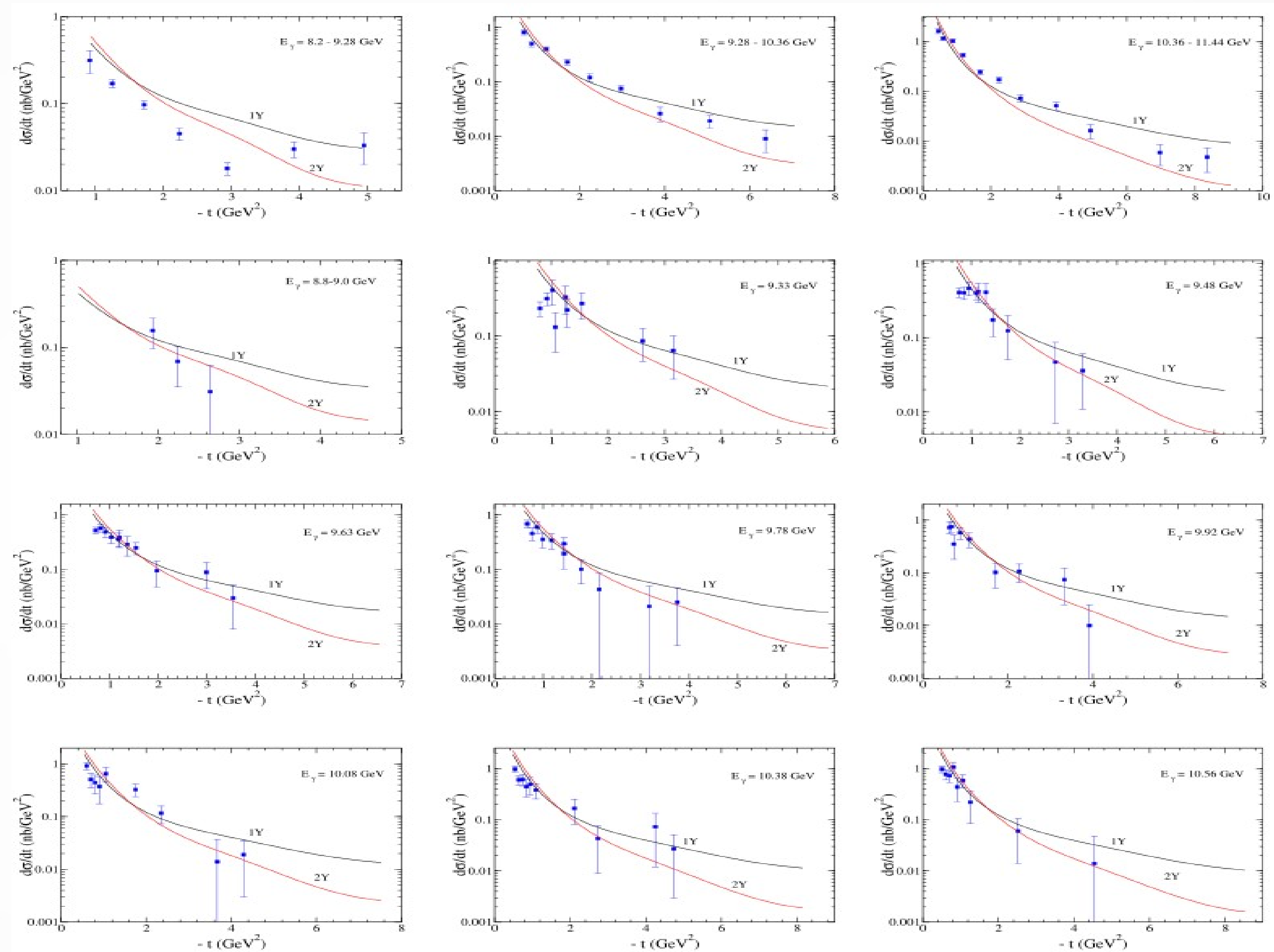

□ The large difference is observed at -t > 2 [GeV^2] between the two models.

□ It originates from the very different short range behaviors of the potential v_{cN} (r).

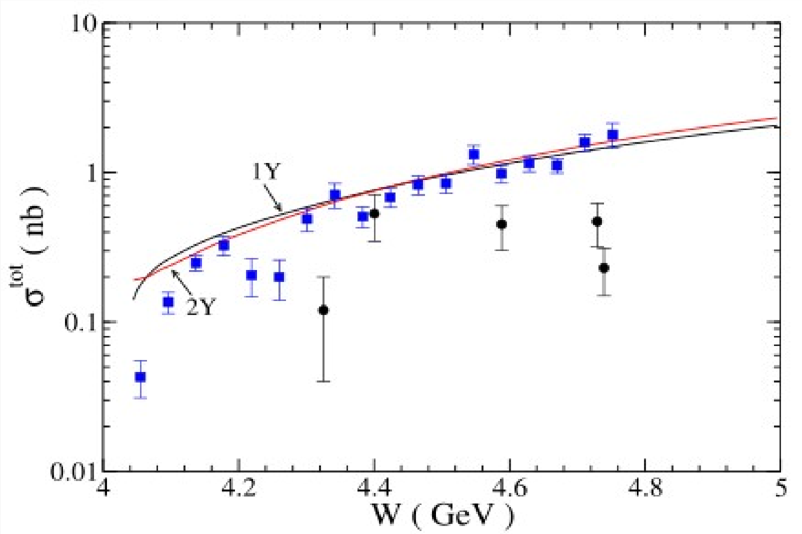

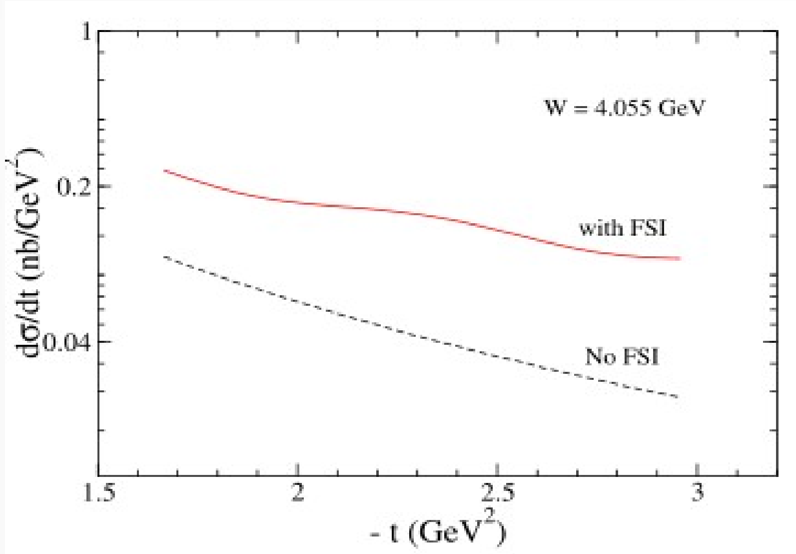

□ The cross sections in the very near threshold region are largely determined by the FSI term.

□ These demonstrate that J/ψ-N interactions can be extracted rather clearly from the J/ψ photoproduction data within this model.

□ More precise data from JLab in the very threshold region and in the large scattering angles are called for.

□ The parametrization of quark-nucleon potential v_{cN} (r) is guided by the Yukawa form extracted from LQCD calculation and must be improved by using more advanced LQCD calculations of J/ψ N scattering, in particular the short-range part of the potential.

□ Talk by S. Sakinah tomorrow in detail

❑ We employ a distorted-wave impulse approximation.

□ Including the FSI term, we can write DCS for spin J=0 nuclei:

$$F_c(q^2) = F_N(q^2)F_T(q^2 = t)$$

F_c (F_N) : nuclear (nucleon) charge FF

$$\frac{d\sigma}{d\Omega_{\rm Lab}} = \frac{(2\pi)^4|\mathbf{k}|^2 E_V(\mathbf{k})E_A(\mathbf{q}-\mathbf{k})}{|E_A(\mathbf{q}-\mathbf{k})|\mathbf{k}| + E_V(\mathbf{k})(|\mathbf{k}| - |\mathbf{q}|\cos\theta_{\rm Lab})|}|AF_T(t)\bar{t}(\mathbf{k},\mathbf{q}) + T^{\rm FSI}(\mathbf{k},\mathbf{q},E)|^2$$

γ ^{4}He → φ ^{4}He

γ p → φ p

$$T(E) = T^{\rm IMP}(E) + T^{\rm FSI}(E)$$

$$T^{\rm IMP} = \sum_{i=1,A}[B_{\phi N_i,\gamma N_i} + T^{N^*}_{\phi N_i,\gamma N_i}]$$

$$T^{\rm FSI}(E) = T_{\phi A,\phi A}(E)\frac{1}{E-H_0}T^{\rm IMP}$$

❑ We employ a distorted-wave impulse approximation.

□ Including the FSI term, we can write DCS for spin J=0 nuclei:

$$\frac{d\sigma}{d\Omega_{\rm Lab}} = \frac{(2\pi)^4|\mathbf{k}|^2 E_V(\mathbf{k})E_A(\mathbf{q}-\mathbf{k})}{|E_A(\mathbf{q}-\mathbf{k})|\mathbf{k}| + E_V(\mathbf{k})(|\mathbf{k}| - |\mathbf{q}|\cos\theta_{\rm Lab})|}|AF_T(t)\bar{t}(\mathbf{k},\mathbf{q}) + T^{\rm FSI}(\mathbf{k},\mathbf{q},E)|^2$$

γ ^{4}He → φ ^{4}He

γ p → φ p

$$F_c(q^2) = F_N(q^2)F_T(q^2 = t)$$

F_c (F_N) : nuclear (nucleon) charge FF

$$T(E) = T^{\rm IMP}(E) + T^{\rm FSI}(E)$$

$$T^{\rm IMP} = \sum_{i=1,A}[B_{\phi N_i,\gamma N_i} + T^{N^*}_{\phi N_i,\gamma N_i}]$$

$$T^{\rm FSI}(E) = T_{\phi A,\phi A}(E)\frac{1}{E - H_0}T^{\rm IMP}$$

γ ^{4}He → J/ψ ^{4}He :

$$T_{\rm total} = T_D + T_{\rm Pom}$$
$$= (B + T_{\rm fsi}) + T_{\rm Pom}$$

$$T_{\rm fsi} = T\frac{1}{W - H_0 + i\epsilon}B$$

❑ We employ a distorted-wave impulse approximation.

$$F_c(q^2) = F_N(q^2)F_T(q^2 = t)$$

F_c (F_N) : nuclear (nucleon) charge FF

□ Including the FSI term, we can write DCS for spin J=0 nuclei:

$$\frac{d\sigma}{d\Omega_{\rm Lab}} = \frac{(2\pi)^4|\mathbf{k}|^2 E_V(\mathbf{k})E_A(\mathbf{q}-\mathbf{k})}{|E_A(\mathbf{q}-\mathbf{k})|\mathbf{k}| + E_V(\mathbf{k})(|\mathbf{k}| - |\mathbf{q}|\cos\theta_{\rm Lab})|} |AF_T(t)\bar{t}(\mathbf{k},\mathbf{q}) + T^{\rm FSI}(\mathbf{k},\mathbf{q},E)|^2$$

γ ^{4}He → J/ψ ^{4}He   γ p → J/ψ p

T_D = B + T_{fsi}

T_{total} = T_D + T_{pom}

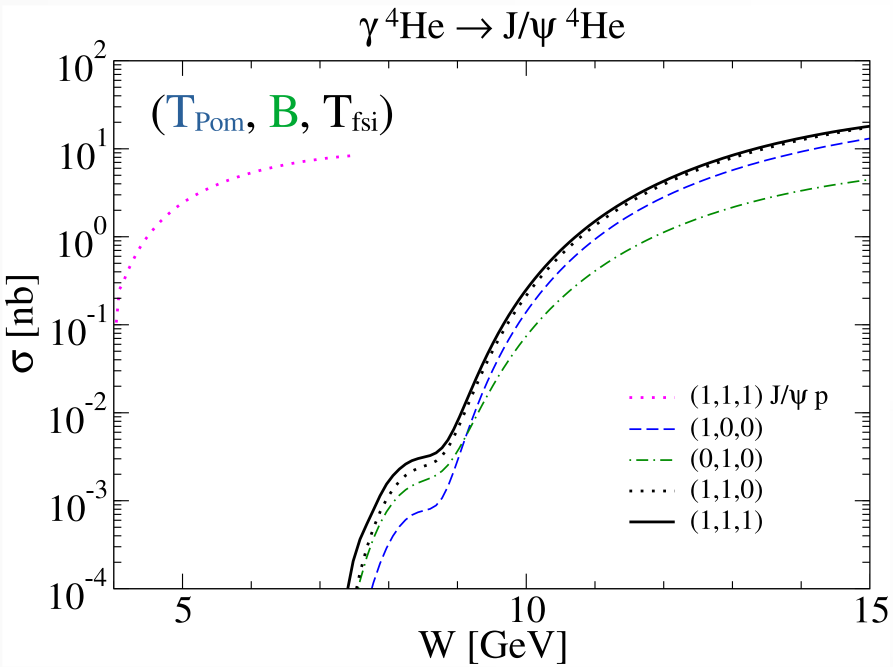

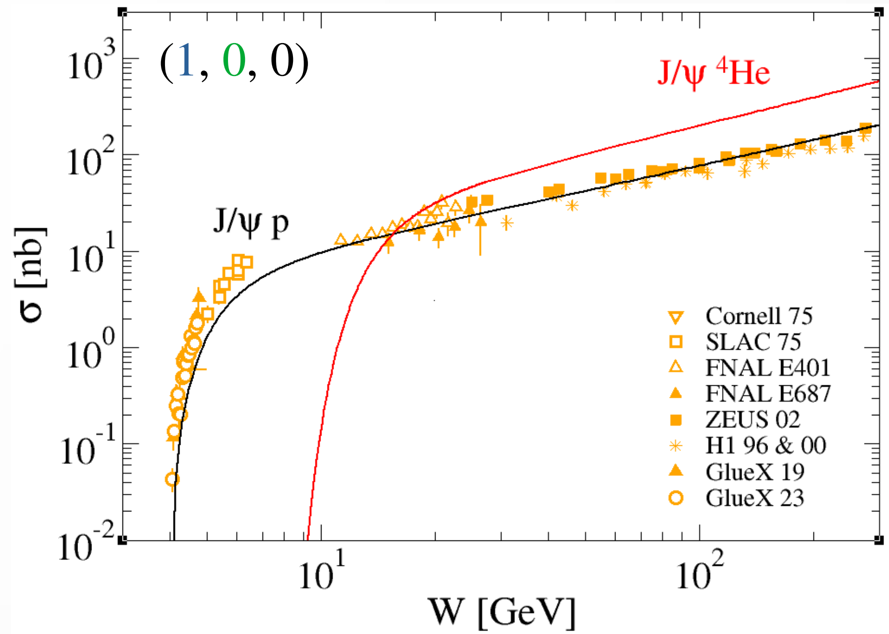

□ The data from EIC and JLab is called for to shed light on the mechanism of J/ψ ^{4}He photoproduction.

□ The dip structures shown at $-t \approx 2$ [GeV^2] are due to the structure of the ^{4}He form factor $F_T(t)$.

□ The FSI contributions are relatively suppressed by factors of about 10^2.

□ The ^{4}He form factor for V18 (Argonne V18) and NV (Norfolk-Verginia) model exhibits rather different shapes at large angles.

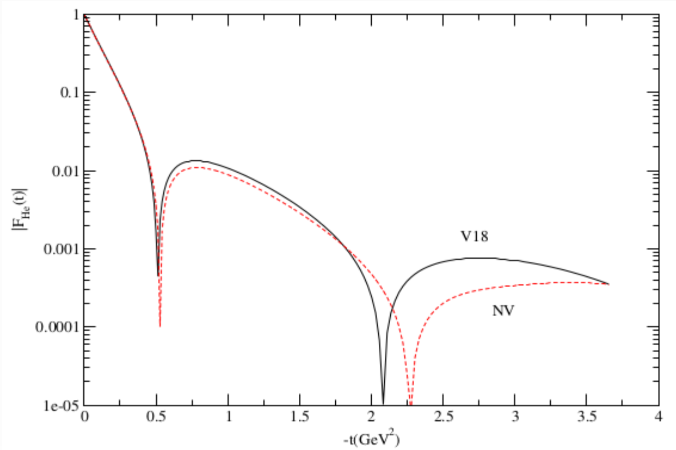

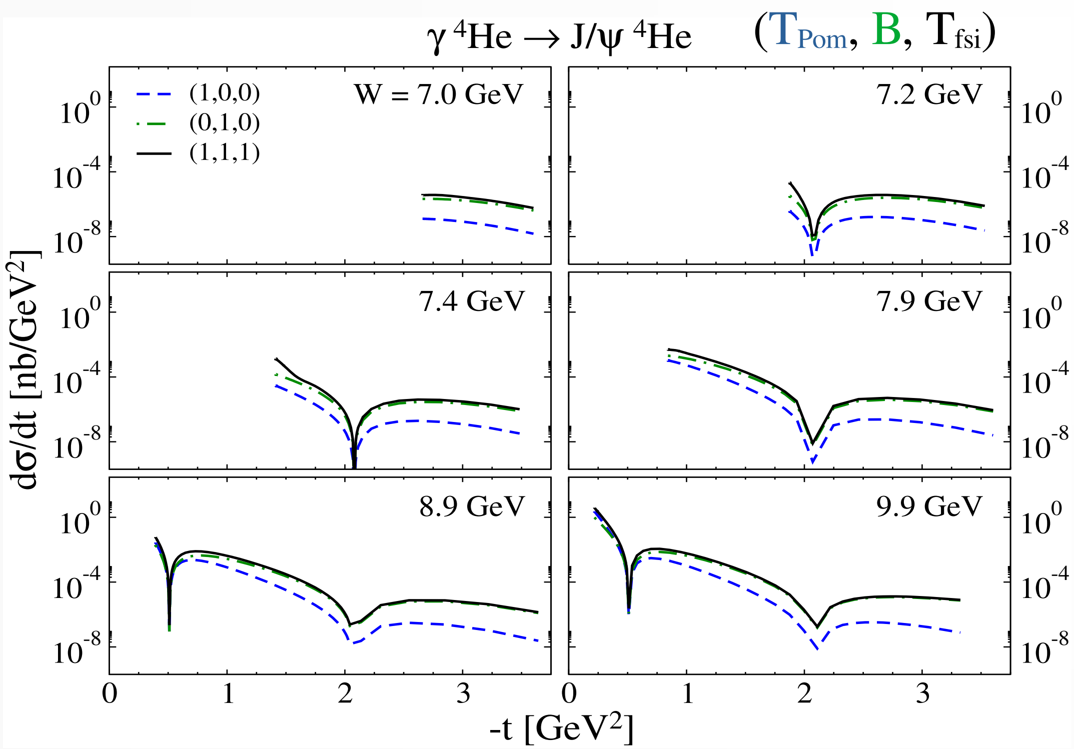

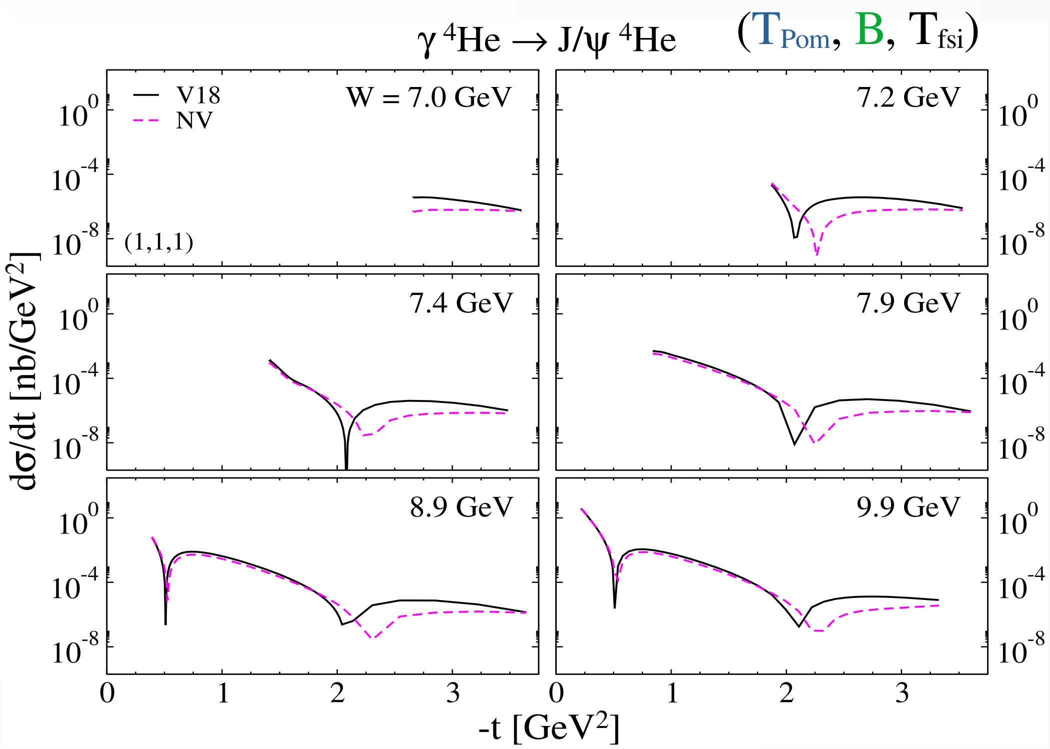

□ The dip structures shown at $-t \approx 2$ [GeV^2] are due to the structure of the ⁴He form factor $F_T(t)$.

□ The FSI contributions are relatively suppressed by factors of about 10^2.

□ The ⁴He form factor for V18 (Argonne V18) and NV (Norfolk-Verginia) model exhibits rather different shapes at large angles.

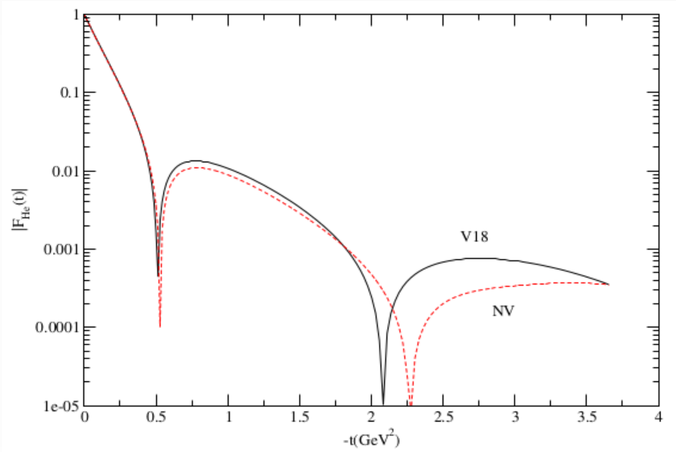

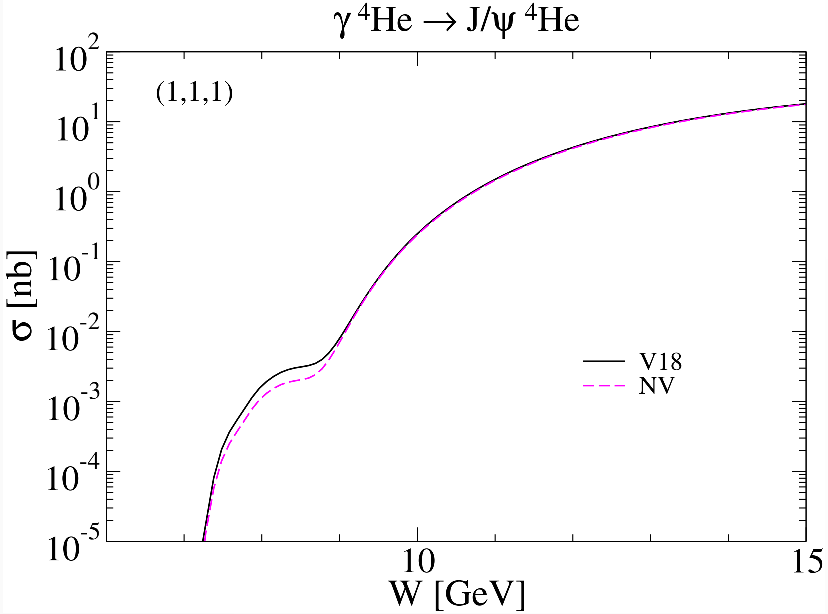

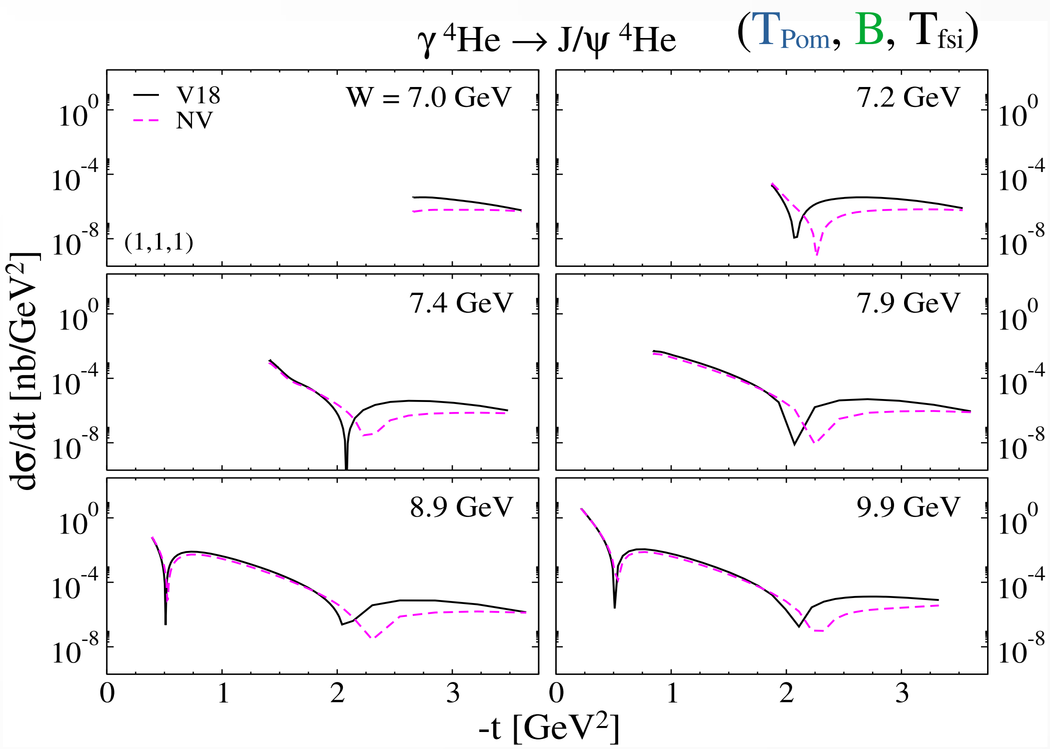

□ With only the total cross section, it is difficult to distinguish the ⁴He form factor used in calculation.

□ For spin J = 1 deuteron, there are two form factors $F_0(k)$ and $F_2(k)$ due to the *s* and *d* wave parts of the deuteron wavefunction, respectively.

□ $F_2(k)$ is due to the crucial tensor force of the NN potential and can be probed by J/ψ exclusive production process clearly.

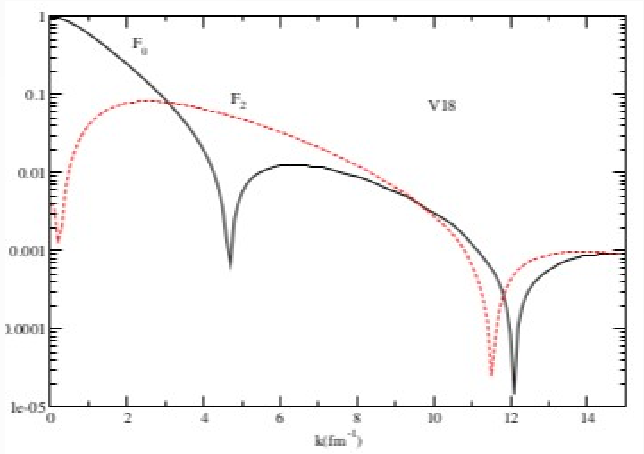

preliminary results

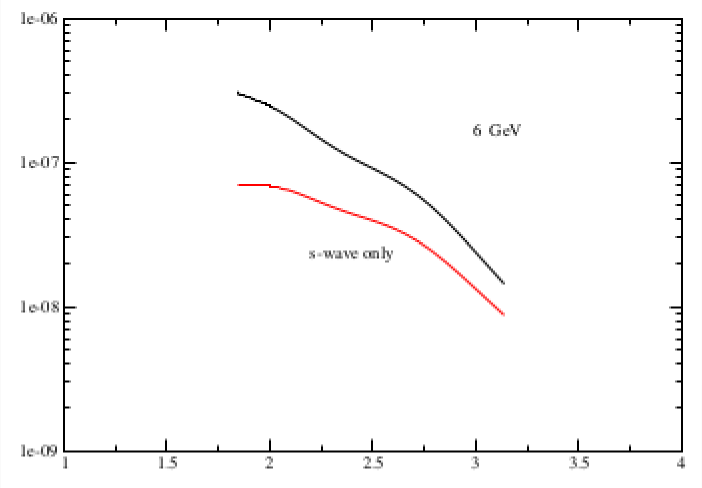

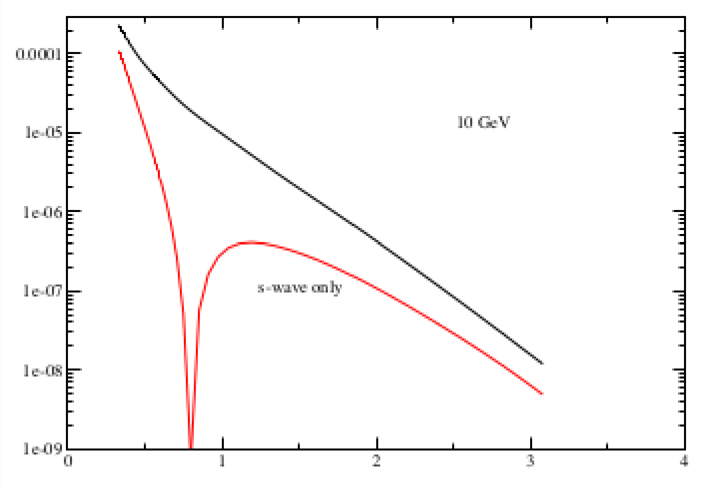

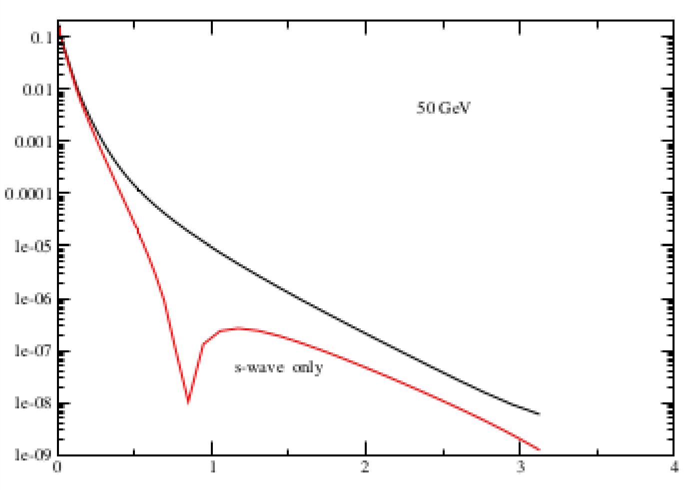

□ The very near threshold covers only large -t regions where the cross sections are mainly due to $F_2(k)$ and thus is very effective in testing the *d*-wave state of deuteron wavefunction.

□ At high energies, small -t regions are also covered such that the dip structure is shown.

□ How do the cross sections depend on the NN model used in generating deuteron wavefunctions?

preliminary results

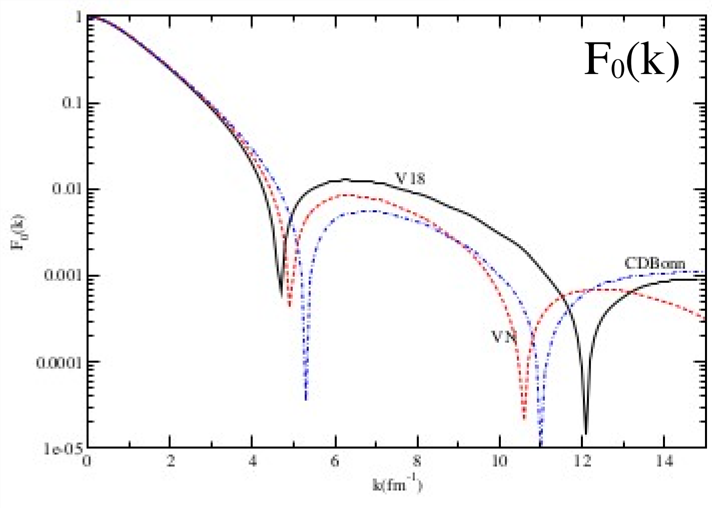

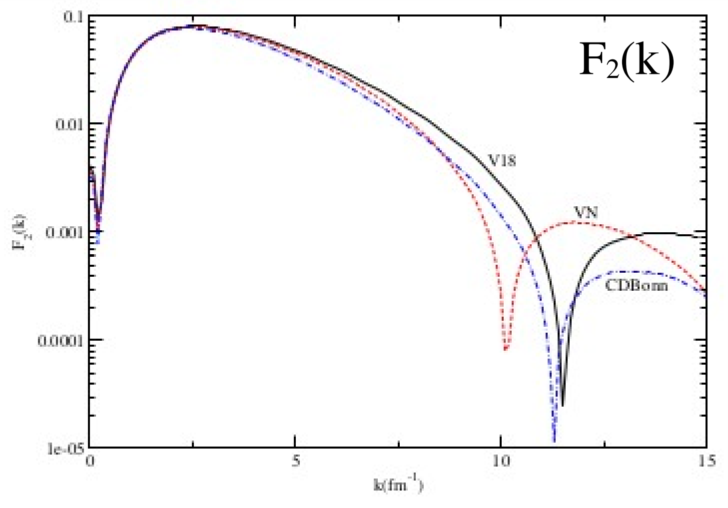

V18 (Argonne V18)
NV (Norfolk-Verginia)
CDBonn

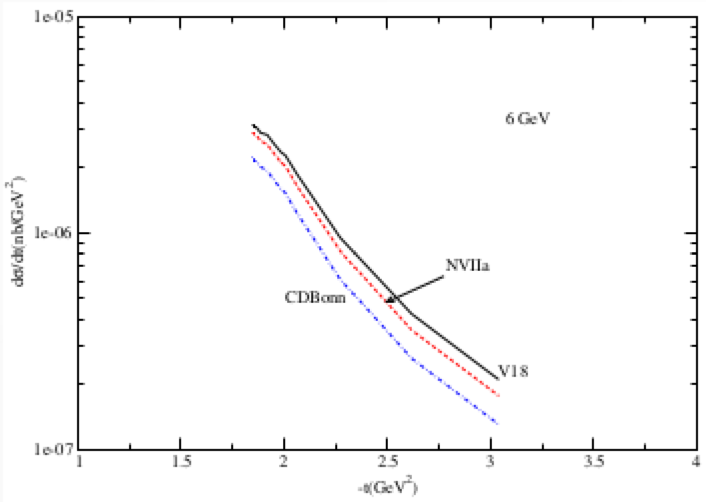

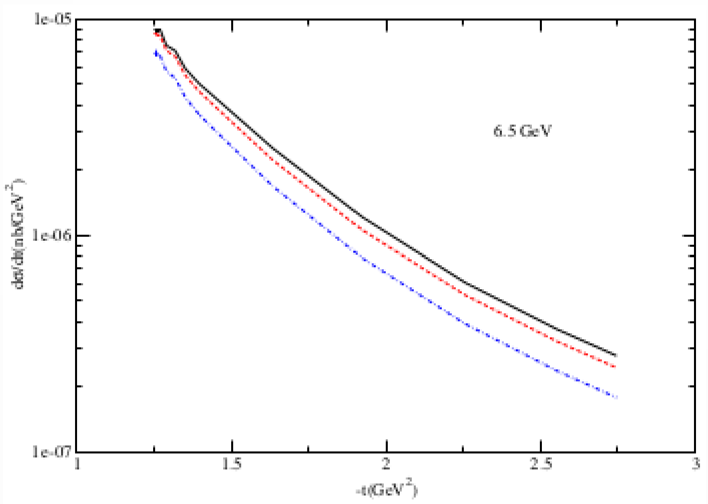

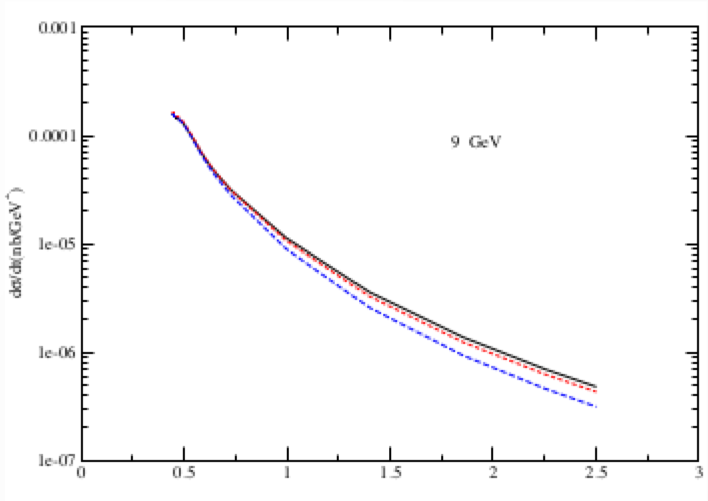

□ They can be distinguished at energies near threshold.

[S.H.Kim, in progress]

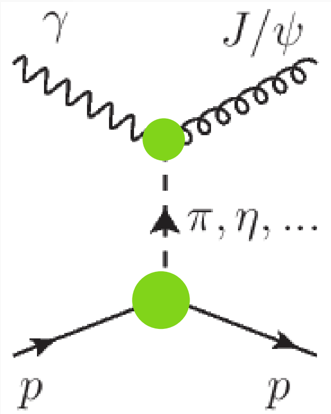

light mesons

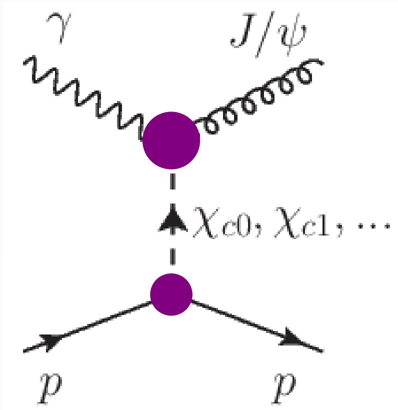

$c\bar{c}$ mesons

- There are many $c\bar{c}$ mesons above J/ψ meson.
- Their contributions may not negligible compared to those of light mesons.
- Which mechanism is more dominant?

$c\bar{c}$ mesons
(including non-$q\bar{q}$ states)

- $\eta_c(1S)$ $0^+(0^{-+})$
- $J/\psi(1S)$ $0^-(1^{--})$
- $\chi_{c0}(1P)$ $0^+(0^{++})$
- $\chi_{c1}(1P)$ $0^+(1^{++})$
- $h_c(1P)$ $0^-(1^{+-})$
- $\chi_{c2}(1P)$ $0^+(2^{++})$
- $\eta_c(2S)$ $0^+(0^{-+})$
- $\psi(2S)$ $0^-(1^{--})$
- $\psi(3770)$ $0^-(1^{--})$
- $\psi_2(3823)$ $0^-(2^{--})$
  was $\psi(3823)$, $X(3823)$
- $\psi_3(3842)$ $0^-(3^{--})$

light mesons

Mesons	Mass (J^P)	$\mathrm{Br}_{J/\psi\to M\gamma}$	$g_{J/\psi\to M\gamma}$	g_{MNN}
π	134 (0^-)	$(3.56 \pm 0.17)\cdot 10^{-5}$	0.002	13.0
η	548 (0^-)	$(1.108 \pm 0.027)\cdot 10^{-3}$	0.011	6.34
η'	958 (0^-)	$(5.25 \pm 0.07)\cdot 10^{-3}$	0.026	6.87
f_1	1285 (1^+)	$(6.1 \pm 0.8)\cdot 10^{-4}$	0.0007	2.5±0.5
$\eta_c(1S)$	2984 (0^-)	$(1.7 \pm 0.4)\cdot 10^{-2}$	2.14	0.0289

$c\bar{c}$ mesons

Mesons	Mass (J^P)	Γ_M [MeV]	$\mathrm{Br}_{M\to J/\psi\gamma}$ [%]	$g_{M\to J/\psi\gamma}$	$\mathrm{Br}_{M\to p\bar{p}}$	$g_{M\to p\bar{p}}$
$\chi_{c0}(1P)$	3415 (0^+)	10.8	1.40 ± 0.05	1.47	$(2.21 \pm 0.08)\cdot 10^{-4}$	0.0046
$\chi_{c1}(1P)$	3511 (1^+)	0.84	34.3 ± 1.0	0.10	$(7.60 \pm 0.34)\cdot 10^{-5}$	0.00084
$\eta_c(2S)$	3638 (0^-)	11.3	< 1.4	< 1.51	seen	–
$\chi_{c1}(3872)$	3872 (1^+)	< 1.2	> 0.7	> 0.008	not seen	–

[S.H.Kim, in progress]

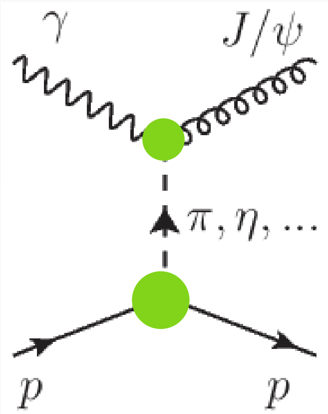

light mesons

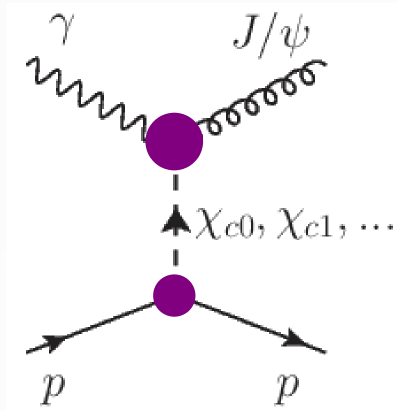

$c\bar{c}$ mesons

Mesons	Mass (J^P)
π	134 (0^-)
η	548 (0^-)
η'	958 (0^-)
f_1	1285 (1^+)
$\eta_c(1S)$	2984 (0^-)

Mesons	Mass (J^P)
$\chi_{c0}(1P)$	3415 (0^+)
$\chi_{c1}(1P)$	3511 (1^+)
$\eta_c(2S)$	3638 (0^-)
$\chi_{c1}(3872)$	3872 (1^+)

- σ (PS mesons) > σ (S mesons) [by one ~ two orders of magnitudes]

- Each Contribution

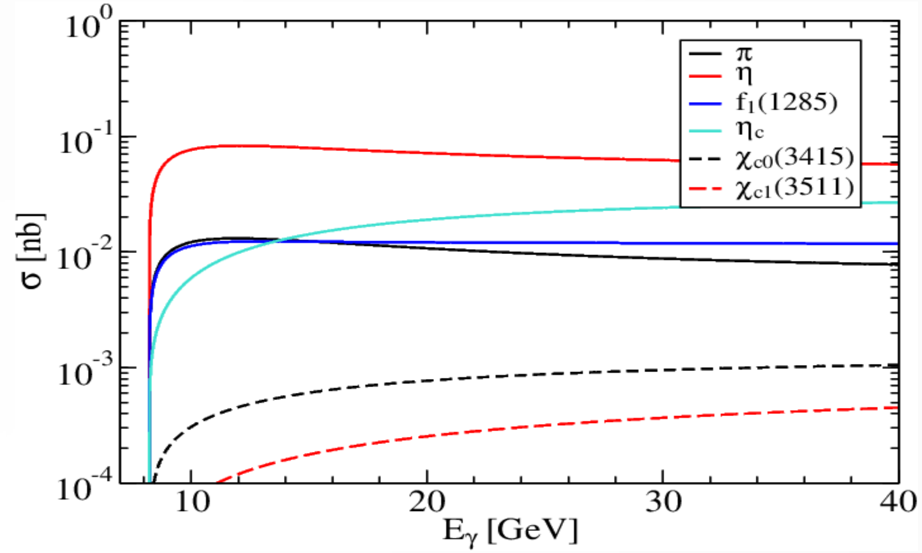

- Total cross section with light mesons included

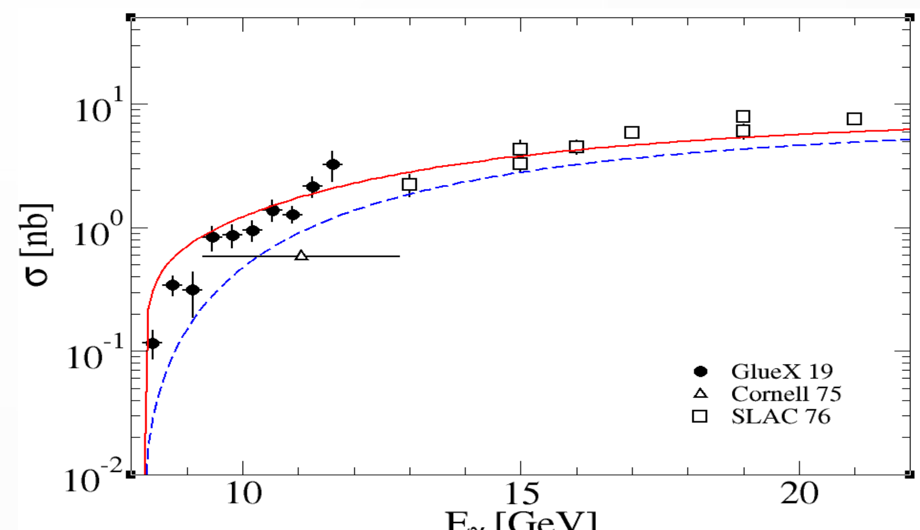

[S.H.Kim, in progress]

$\gamma^* p \rightarrow \varphi p$ [S.H.Kim, PRC.101.065201 (2020)]

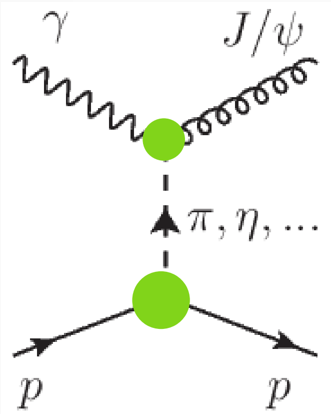

σ (PS mesons)

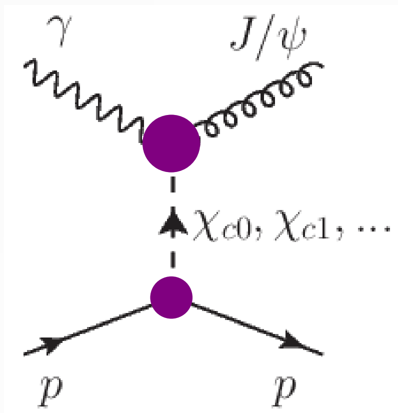

σ (S mesons)

← dominant →

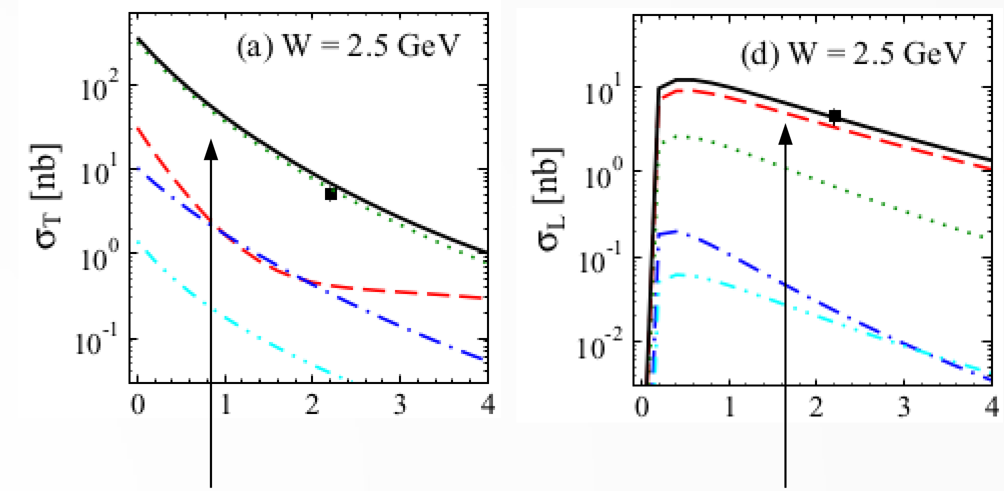

Pomeron

Scalar meson

- The dominant mechanism can be verified by the future EIC and JLab data for the spin polarization observables, e.g., beam asymmetry.

- In vector-meson (φ) electroproduction, $\gamma^* p \rightarrow \varphi p$, we know that S-meson plays an important role at low W and low Q^2 for σ_L.

$$\frac{d\sigma}{d\Phi} = \frac{1}{2\pi}\left(\sigma + \varepsilon\sigma_{TT}\cos 2\Phi + \sqrt{2\varepsilon(1+\varepsilon)}\sigma_{LT}\cos\Phi\right) \quad \sigma = \sigma_T + \varepsilon\sigma_L$$

- The role of $\chi_{c0}(3415,0^+)$ can be found from the future EIC and JLab data for $\gamma^* p \rightarrow J/\psi\, p$ reaction at low W and low Q^2.

□ Two pronounced cusp structures are located at the $\bar{D}\Lambda_c$ and $\bar{D}^*\Lambda_c$ thresholds.

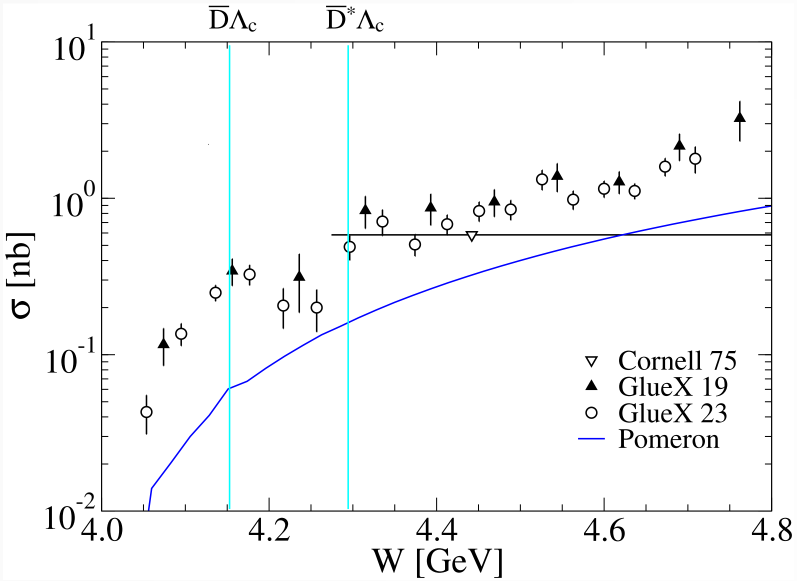

$$\mathcal{L}_{\Lambda_c DN} = -g_{D^*N\Lambda_c}\bar{\Lambda}_c\gamma_\mu N D^{*\mu} - ig_{DN\Lambda_c}\bar{\Lambda}_c\gamma_5 N D$$
$$-g_{D^*N\Lambda_c}\bar{N}\gamma_\mu\Lambda_c D^{*\mu\dagger} - ig_{DN\Lambda_c}\bar{N}\gamma_5\Lambda_c D^\dagger,$$

$$\mathcal{L}_\psi = -g_{\psi DD^*}\psi_\mu\epsilon_{\mu\nu\alpha\beta}\left(\partial_\nu D^*_\alpha\partial_\beta D^\dagger - \partial_\nu D\partial_\beta D^{*\dagger}_\alpha\right),$$
$$+ig_{\psi D^*D^*}\psi^\mu\left(D^{*\nu}\partial_\nu D^{*\dagger}_\mu - \partial_\nu D^*_\mu D^{*\nu\dagger}\right.$$
$$\left.-D^{*\nu}\overleftrightarrow{\partial}_\mu D^{*\dagger}_\nu\right) - ig_{\psi DD}D^\dagger\overleftrightarrow{\partial}_\mu D\psi^\mu$$
$$+g_{\psi\Lambda_c\Lambda_c}\bar{\Lambda}_c\gamma_\mu\psi^\mu\Lambda_c,$$

$$\mathcal{L}_\gamma = -g_{\gamma DD^*}F_{\mu\nu}\epsilon^{\mu\nu\alpha\beta}(D^*_\alpha\overleftrightarrow{\partial}_\beta D^\dagger - D\overleftrightarrow{\partial}_\beta D^{*\dagger}_\alpha)$$
$$-ig_{\gamma D^*D^*}F^{\mu\nu}D^{*\dagger}_\mu D^*_\nu - e\bar{\Lambda}_c\gamma_\mu A^\mu\Lambda,$$

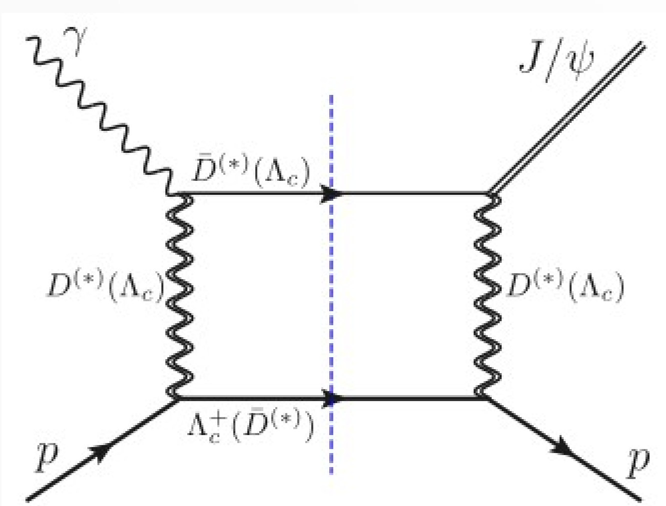

Coupling	$g_{\gamma DD^*}$	$g_{\gamma D^*D^*}$	$g_{DN\Lambda_c}$	$g_{D^*N\Lambda_c}$	$g_{\psi\Lambda_c\Lambda_c}$	$g_{\psi DD}$
Value	0.134 GeV^{-1}	0.641	−4.3	−13.2	−1.4	7.44
Source	Experimental data [46]		SU(4) [47,48]			VMD [47,48]

□ The presence of such cusps can be a clear indication of the importance of the charm loops.

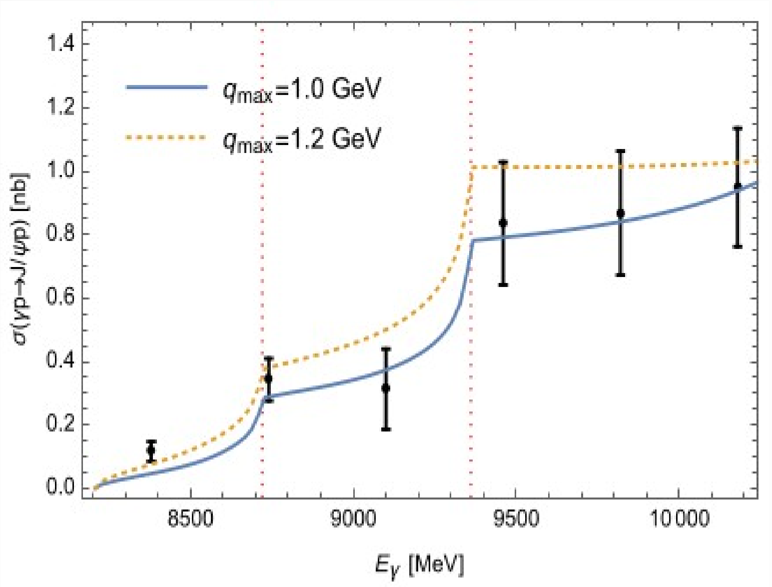

[Du, EPJC.80.1053 (2020)]

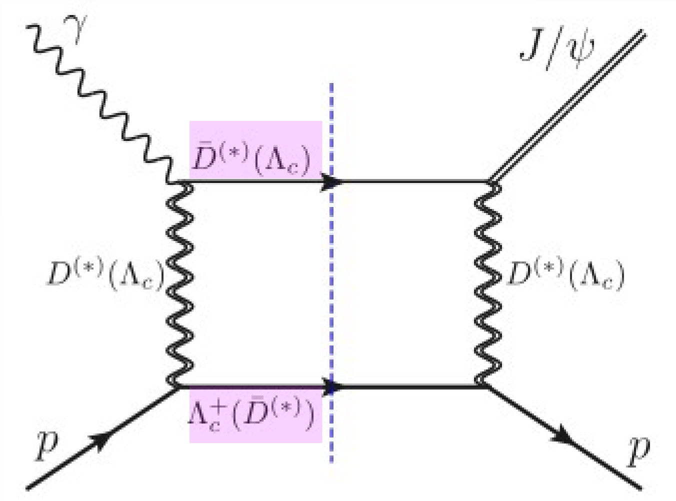

□ We calculate
$\bar{D}\Lambda_c$: 3 terms
$\bar{D}^*\Lambda_c$: 5 terms

□ We are trying to calculate this region by using the 3-dimensional reduction of the Bethe-Salpeter equation for both principal and singular parts.

$$T_{MB}(p,p') = \sum_i \int \frac{d^3\mathbf{q}}{(2\pi)^3} \frac{m_{B_i}}{E_{B_i}} T_{\gamma p \to M_i B_i}(p,q) \frac{1}{s-(E_{M_i}+E_{B_i})^2+i\epsilon} T_{M_i B_i \to J/\psi p}(q,p')$$

$$= -i \sum_i \frac{q_{\mathrm{c.m.}}}{16\pi^2} \frac{m_{B_i}}{\sqrt{s}} \int d\Omega \left[T_{\gamma p \to M_i B_i}(p,q) T_{M_i B_i \to J/\psi p}(q,p')\right] + \mathcal{P}$$

◇ For $\gamma\, p \to \varphi\, p$,
we studied relative contributions between the Pomeson and various meson exchanges.
> The light-meson (π, η, a_0, f_0,...) contribution is crucial to describe the data at low energies.

The final φN interactions are described by the gluon-exchange, direct φN couplings, and the box diagrams arising from the couplings with πN, ρN, $K\Lambda$, and $K\Sigma$ channels. > suppressed by $10^2 - 10^3$.

◇ For $\gamma\, {}^4He \to \varphi\, {}^4He$,
a distorted-wave impulse approximation is employed within the multiple scattering formulation.
> The FSI effects are suppressed compared to the Born term by $10^1 - 10^3$.

◇ For $\gamma\, p \rightarrow \varphi\, p$,
we studied relative contributions between the Pomeson and various meson exchanges.
> The light-meson (π, η, a_0, f_0,...) contribution is crucial to describe the data at low energies.

The final φN interactions are described by the gluon-exchange, direct φN couplings, and the box diagrams arising from the couplings with πN, ρN, $K\Lambda$, and $K\Sigma$ channels. > suppressed by $10^2 - 10^3$.

◇ For $\gamma\, {}^4He \rightarrow \varphi\, {}^4He$,
a distorted-wave impulse approximation is employed within the multiple scattering formulation.
> The FSI effects are suppressed compared to the Born term by $10^1 - 10^3$.

◇ We suggested three models for $\gamma\, p \rightarrow J/\psi\, p$:
dynamical model, meson-exchange model, Box-diagram model

◇ Based on the two dynamical models, we investigated $\gamma\, A \rightarrow J/\psi\, A$ ($A = d$, ${}^4He$, ${}^{12}C$, ${}^{16}O$, ${}^{40}Ca$) reaction.

◇ For both $\varphi\, p$ and $J/\psi\, p$ photoproduction, the meson-baryon loops seem to be the dominant processes rather than the pentaquark (P_s, P_c) contributions in the *s* channel.

◇ We will improve our model to relate the phenomenological c quark-nucleon potential to gluon GPD in nucleon, such that the gluon distributions in nuclei can be predicted for EIC experiments.

◇ Approved 12 GeV era experiments to date at Jafferson Labarotory:

[E12-09-003] Nucleon Resonances Studies with CLAS
[E12-11-005] Meson spectroscopy with low Q^2 electron scattering in CLAS12
[E12-12-006] Near Threshold Electroproduction of J/ψ at 11 GeV
[E12-12-007] Exclusive Phi Meson Electroproduction with CLAS12

◇ We will improve our model to relate the phenomenological c quark-nucleon potential to gluon GPD in nucleon, such that the gluon distributions in nuclei can be predicted for EIC experiments.

◇ Approved 12 GeV era experiments to date at Jafferson Labarotory:
[E12-09-003] Nucleon Resonances Studies with CLAS
[E12-11-005] Meson spectroscopy with low Q^2 electron scattering in CLAS12
[E12-12-006] Near Threshold Electroproduction of J/ψ at 11 GeV
[E12-12-007] Exclusive Phi Meson Electroproduction with CLAS12

Thank you very much for your attention